



**University of  
Zurich**<sup>UZH</sup>

# Impact of climate change on dew formation

ESS 511 Master's Thesis

**Author**

Muriel Stefanie Trüb  
17-110-081

**Supervised by**

Dr. Vincent Humphrey (vincent.humphrey@env.ethz.ch)  
Dr. Erich Fischer (erich.fischer@env.ethz.ch)  
Prof. Dr. Alexander Damm

**Faculty representative**

Prof. Dr. Alexander Damm

30.09.2022

Department of Geography, University of Zurich



University of  
Zurich <sup>UZH</sup>

**ETH**

Eidgenössische Technische Hochschule Zürich  
Swiss Federal Institute of Technology Zurich

# Impact of climate change on dew formation

Master Thesis

University of Zürich

Earth System Science

Department of Geography

ETH Zürich

Institute for Atmospheric and Climate Science

Department of Environmental Systems Science

and Department of Earth Sciences

Submitted by:

**Muriel Trüeb**

September 2022

Supervised by:

Dr. Vincent Humphrey <sup>1</sup>

Dr. Erich Fischer <sup>1</sup>

Prof. Dr. Alexander Damm <sup>2</sup>

<sup>1</sup> Institute for Atmospheric and Climate Science, ETH Zürich

<sup>2</sup> Institute of Remote Sensing, Department of Geography, University of Zürich



---

## Contents

<b>Abstract</b>	<b>i</b>
<b>1 Introduction and Background</b>	<b>1</b>
1.1 Introduction . . . . .	1
1.2 Background . . . . .	2
1.3 Objectives . . . . .	4
<b>2 Data and Methods</b>	<b>4</b>
2.1 Data . . . . .	4
2.1.1 CMIP6 data . . . . .	4
2.1.2 Satellite and in situ data . . . . .	5
2.2 Methods . . . . .	6
2.2.1 Dew point temperature . . . . .	7
2.2.2 Definition of the number of dew days . . . . .	8
2.2.3 Evaluation and bias-correction . . . . .	10
2.2.4 Post-processing . . . . .	15
<b>3 Results and Discussion</b>	<b>16</b>
3.1 Climatology of estimated number of dew days . . . . .	16
3.2 Global change in estimated dew days . . . . .	20
3.2.1 Global trend in estimated dew days . . . . .	20
3.2.2 Global patterns and model differences . . . . .	23
3.2.3 Global patterns relative to counted days . . . . .	25
3.3 Zonal and regional trends in estimated dew days . . . . .	30
3.3.1 Changes in the zonal mean . . . . .	30
3.3.2 Impact of different biomes on dew frequency . . . . .	33
3.3.3 Seasonality in the Amazon . . . . .	38
<b>4 Conclusion</b>	<b>43</b>
<b>5 Outlook</b>	<b>46</b>
<b>6 Acknowledgment</b>	<b>47</b>
<b>References</b>	<b>48</b>
<b>7 Appendices</b>	<b>53</b>



---

## Abstract

Dew is a relatively small but essential part of the water cycle that is associated with the global climate. It forms by condensing of atmospheric water vapor on surfaces when the surface temperature drops below dew point temperature ( $T_d$ ). The small droplets of water can help to compensate for precipitation. Especially in dry areas, it is an important contribution to the water supply. Even though in situ measurements expect dew formation to change in future climate, there is little information from climate model projections on a global scale. Most of the former model outputs of the CMIP archive did not provide the needed variables in a high temporal resolution so that it would be possible to analyze changes in dew formation. With newly available three-hourly data model outputs within CMIP6, it is possible to analyze the change in favorable conditions for dew formation for the first time. We analyze climate model outputs from 1950-2100 with the ssp585 scenario to assess the global change in favorable conditions for dew formation with the changing climate. The following questions are discussed: *i.* Does the number of days that are favorable to dew formation change with warmer temperatures? *ii.* Is there a robust change in dew formation among models? *iii.* In which climate zones will dew formation be most sensitive to changing conditions? *iv.* Is the change in estimated dew days related to biomes? *v.* Is there a seasonal tendency in dew formation in the Amazon?

The findings will help to understand the impact of projected climate change on favorable atmospheric conditions for dew formation and assess the sensitivity of different regions.

Outputs of six different models within the CMIP6 archive are analyzed. Only outputs of the high forcing scenario ssp585 are included. Since there is no variable indicative of dew, we analyze the change in favorable atmospheric conditions for dew formation. Our results show that warm regions with high relative humidity show a high number in estimated dew days; in contrast, areas with lower relative humidity during the day depend more on the amplitude of the diurnal temperature cycle. With changing climate, the global mean of the estimated number of dew days increases. The increase is partly due to the increasing number of days with temperatures above 0°C in the North. The increasing trend is not reflected everywhere; there are different regional patterns in the estimated change of dew days. The increase in large parts of the Northern Hemisphere stays in contrast to the decrease in the Southern Hemisphere. A robust increase among the six models is located in the northern high latitudes, part of central Asia, and parts of North America. The increase in Eurasian high-latitudes could be influenced by a higher amplitude in the diurnal temperature in the future. In the Amazon, Congo Basin, central Europe, and parts of Southeast Asia, there is a robust decrease in the estimated number of dew days. The projected decrease in the tropics may be caused by the decrease in relative humidity.

The biomes predominant in the North show an increase in the number of estimated dew days. Extratropical forests seem more sensitive to the increasing number of days with temperatures above freezing point than other biomes dominant in the North. In contrast to the North, evapotranspiration seems to influence biomes associated with dry and warm conditions. With the warming in the future, the atmospheric dryness could increase due to lower stomatal activity. This could cause less favorable conditions for dew formation in semiarid ecosystems compared to sparsely vegetated dry areas. Tropical forests show a strong decrease in the estimated dew frequency. The drivers of changes in these regions, especially in the Amazon, are difficult to assess since this is a complex system that is self-feeding due to a high precipitation recycling rate.

Overall, one can conclude that the number of estimated dew days increases in the Northern Hemisphere and decreases in the Southern Hemisphere. More frequent dew days on northern agricultural land may lead to lower crop yield. Dew decrease in semiarid ecosystems seems to enhance drying and warming in these areas. The first attempt to assess dew changes with future climate emphasizes the importance of including dew as a variable in a future climate model.

# 1 Introduction and Background

## 1.1 Introduction

The global distribution of water is a complex cycle crucial to life in all forms. Dew is associated with this cycle as part of the condensation and precipitation process. Unlike rain and snow, dew forms on the surface when the surface temperature ( $T_s$ ) drops below the dew point temperature ( $T_d$ ).  $T_d$  indicates the temperature at which the air becomes fully saturated with water vapor. In other words, dew can precipitate when the maximum water holding capacity of air is reached at the surface.

Precipitation in the form of dew is an important contribution to the water supply in many dry areas (Kidron and Starinsky, 2019), especially during the dry season. For instance, dew accounts for 50% of the annual precipitation in the Taklimakan desert in China (Hao et al., 2012). Hao et al. (2012) showed that in some years, dew fall during summer can supply the ecosystem with more water than precipitation does. Moreover, dew contributes up to 30% to the annual water input in semi-arid areas (Aguirre-Gutiérrez et al., 2019).

In such areas, human inventions can help to overcome dry periods by using dew collectors to increase the water supply for agricultural purposes, reforestation (Tomaszkiewicz et al., 2017), or even as contribution to residential use (Lekouch et al., 2012; Sharan, 2007). Indeed, Vuollekoski et al. (2015) concluded that dew harvesting has a high potential for water supply in rather dry areas. This indicates that dew can be an important part of the water cycle, especially in water-stressed regions.

Dew is not only crucial to ecosystems in dry regions, but it can also play an important role in leaf canopy wetness in the tropics, where foliar water uptake can reduce water stress (Berry et al., 2019) in dry seasons. For instance, in the Eastern Amazon 20% of the annual canopy wetness is due to dew (Binks et al., 2021).

Although dew can positively impact the water supply in some regions, it can also have a negative effect in other regions. For example, the thin water film on the surface of plants can enhance diseases and pests in plants. This can reduce crop yield (Nath, 2021; Agam and Berliner, 2006).

Besides the water cycle, dew formation also depends on the energy budget. Dew forms at night when net radiation is negative, and radiative cooling can occur (Garratt and Segal, 1988). This process allows the surface temperature ( $T_s$ ) to reach values below  $T_d$ . In humid air  $T_d$  is reached faster than in dry air, since  $T_d$  depends on the atmosphere's water vapor content. However, surface cooling is reduced by very high atmospheric water vapor in the boundary layer (Ritter et al., 2019). Because water vapor acts as a greenhouse gas, it increases downwelling long-wave radiation, which

then counteracts radiative cooling of the surface. When radiative cooling is inhibited,  $T_s$  does not drop below  $T_d$ , thus preventing dew formation. This means that the atmospheric water content affects nighttime surface cooling, which itself is also a driver of dew formation.

In summary, the atmospheric conditions for dew formation are favorable when the surface temperature drops below dew point temperature ( $T_s \leq T_d$ ), i.e., the point when the air is fully saturated with water (Aguirre-Gutiérrez et al., 2019; Dou et al., 2021; Ritter et al., 2019; Wang et al., 2017; Yu et al., 2020). According to an empirical study, the probability of dew formation already starts to increase linearly when relative humidity at two meter height is above 73% (Aguirre-Gutiérrez et al., 2019). Ritter et al. (2019) even state that it is more favorable to have relative humidity below 100%, since a too high atmospheric water content inhibits surface cooling. Also, high wind speed disturbs dew forming (Ritter et al., 2019; Wang et al., 2017; Yu et al., 2020). Since wind induces air mixing, it inhibits stratification and can lead to drier conditions.

Besides atmospheric states, local-scale characteristics, such as elevation (Pütz et al., 2016), orientation to the sun (Kidron, 2000), surface characteristics, and canopy characteristics of the vegetation (Binks et al., 2021; Ritter et al., 2019; Wang et al., 2017) as well as plants or soil moisture (Garratt and Segal, 1988; Pütz et al., 2016), affect dew formation (Yu et al., 2020). Where the latter must be separated from atmospheric dew formation, guttation (plant water loss) and dew rise (evaporation from the soil) are effects that are not considered in this thesis since they are based on small-scale land surface properties instead of atmospheric conditions.

## 1.2 Background

With climate change, temperatures are increasing, and the water content in the atmosphere is changing (Dunn et al., 2017; Feng and Fu, 2013; Simmons et al., 2010; Dai, 2006). The water holding capacity of the atmosphere depends on pressure and temperature. The relationship between the two variables shows that the air can contain more water vapor with increasing temperature. This results in an increase in specific humidity. According to O’Gorman and Muller (2010), there is an increase of  $7.3\% \text{ K}^{-1}$  in specific humidity, closely following the Clausius-Clapeyron equation. However, if only the bottom layer of the atmosphere over land areas is considered, the specific humidity does not increase as much ( $5.9\% \text{ K}^{-1}$ ). The lower increase in specific humidity is assumed to be due to faster increasing temperatures over land. If the amount of water vapor close to the surface increases more slowly with increasing surface temperature, the dew point temperature is less likely to be reached, reducing favorable conditions for dew formation at night.

In contrast to specific humidity, relative humidity (RH) decreases with increasing temperatures (Sim-

mons et al., 2010), particularly over land areas. This is partly because temperatures over land areas increase faster than over oceans. Therefore, the same amount of specific humidity equals lower relative humidity over land than over the ocean since there are warmer temperatures. In other words, the relative humidity decreases over land because the warmer temperatures over the continents have a higher water holding capacity than over the ocean (Sherwood and Fu, 2014).

Increasing atmospheric dryness is often expressed by the ratio of precipitation to potential evapotranspiration (P/PET). This ratio is used as a quantitative index for atmospheric dryness in a location. Studies use the P/PET ratio to show the expansion of drylands with increasing temperature (Feng and Fu, 2013). Even though it is still an ongoing debate if this method is well suited for vegetation change or not (Berg and McColl, 2021), the ratio can be used as an indicator for background dryness (Sherwood and Fu, 2014). Other studies emphasize that with higher CO<sub>2</sub> fertilization of plants, their water use efficiency increases which would counteract the drying in soil moisture (Berg and McColl, 2021). Higher CO<sub>2</sub> fertilization also means less stomatal activity and, thus, less transpiration (Berg and McColl, 2021), which leads to a drying of the atmosphere (Berg et al., 2016). Additionally, water-stress also diminishes the stomatal activity. Low soil moisture during dry spells reduces carbon uptake (Humphrey et al., 2021).

With increased temperatures, less dew occurrence is expected in dry grassland (Feng et al., 2021). However, there is only little information about projections of dew formation on a global scale. Some studies suggest that dew formation will likely be affected by climate change, as it mainly depends on (near) surface temperature and relative humidity (RH) (Dou et al., 2021). Few observational studies of dew formation have been conducted in different regions.

Although the in situ studies agree on the negative effect of the changing climate on dew fall (Dou et al., 2021; Feng et al., 2021), there is little information from climate model projections about dew on a global scale. Dew is not even a part of the latest reports of the Intergovernmental Panel on Climate Change (IPCC, 2021). Due to the lack of high temporal resolution outputs in earlier Coupled Model Intercomparison Projects (CMIP), the change in dew formation could not be analyzed yet, although it is a crucial component of the land water balance for some areas. However, in the most recent CMIP projections, CMIP6, a larger number of models provide three-hourly data. This allows us to investigate changes in conditions favorable to dew formation for the first time.

There is no modeled variable indicative for dew formation. Therefore, dew days are estimated based on dew point temperature. It is a first approach in investigating favorable atmospheric conditions for dew formation, based on the newly available high resolution data outputs of the climate models from the CMIP6 archive.

### 1.3 Objectives

In this master's thesis, the newly available climate projections for 1950 to 2100 are used to understand how dew will be affected by climate change. It is assessed whether favorable conditions for dew formation will change. This master's thesis discusses the following questions:

- i. Does the number of days favorable to dew formation change with warmer temperatures?
- ii. Is there a robust change in dew formation among models?
- iii. In which climate zones will dew formation be most sensitive to changing conditions?
- iv. Is the change in estimated dew days related to biomes (tropical forests, etc.)?
- v. Is there a seasonal tendency in dew formation in the Amazon?

The findings will indicate the importance of dew in future climate and help to detect regions in which dew is more sensitive to climate change, regarding the frequency of the conditions favorable to dew fall.

## 2 Data and Methods

### 2.1 Data

The used data for the analysis is described in this section. First, the model data is defined, then the satellite data and observation studies are listed.

#### 2.1.1 CMIP6 data

Since the Earth system is very complex but crucial to understand, climate models have become fundamental tools in climate science to understand past, present, and future climate. Models within the Coupled Model Intercomparison Project (CMIP) are based on a standardized framework so that the model outputs can be intercompared, and a multi-model mean can then be used as a basis for more robust results (Eyring et al., 2016). The model outputs are the basis for *the Intergovernmental Panel on Climate Change (IPCC)* reports which assess the status of scientific knowledge on climate change with regard to the expected dangers and proposals of mitigation (see <https://www.ipcc.ch/>).

In this master's thesis, CMIP6 model outputs are used to assess the impact of climate change on dew formation. We focus on the atmosphere model outputs with historical runs and a future projection with induced predefined CO<sub>2</sub> forcing. Six models of the CMIP6 archive are analyzed. The models are listed in Tab. 1. Other models were excluded because only the six selected models saved the variables

in the required three-hourly resolution.

The *r1i1p1f1* ensemble and the sheared socio-economic pathway 5-8.5 (ssp585) is selected for this analysis. ssp585 is the pathway with a slow development in environmentally sustainable technology. In this plot, the economy will rely on fossil fuel which leads to a high forcing scenario (Meinshausen et al., 2020). It is often referred to as business as usual.

Three-hourly resolved data from 1950 to 2100 is taken into account, with the variables expressed in a three-hourly mean of a grid cell. The spatial resolution is between  $0.7^\circ$  to  $1.25^\circ$  and  $0.7^\circ$  to  $1.875^\circ$  in latitude and longitude, respectively (Tab. 1). Models within CMIP6 do not provide a variable indicative of dew formation. Therefore, one can only estimate favorable atmospheric conditions of dew formation based on other variables. The variables used to determine these conditions are surface air temperature (*tas*), surface specific humidity (*huss*), and surface pressure (*ps*), whereas *surface* indicates the level two meters above roughness level.

Please note that surface air temperature (*tas*) is used instead of surface skin temperature ( $T_s$ ), since  $T_s$  is not available in most models. Although the deviation of *tas* from  $T_s$  is a limitation, it is a reasonable approximation in our case because favorable conditions will be analyzed instead of actual dew formation. In addition, the surface air temperature is corrected based on an evaluation that has been performed (shown in Section 2.2.3). Additional to the above listed variables (*tas*, *huss*, and *ps*), three-hourly resolved precipitation (*pr*) is included in the analysis.

### 2.1.2 Satellite and in situ data

Satellite data of MODIS is used for land cover information (Friedl and Sulla-Menashe, 2015). The land cover classification is based on the Leaf Area Index (LAI) of MCD12C1 (Sulla-Menashe and Friedl (2018), Tab. 5) and summarized into the following six ecosystem types based on Ahlström et al. (2015): Forest between  $24^\circ\text{S}$  and  $24^\circ\text{N}$  is classified as tropical forest. Outside this boundary, it is classified as an extratropical forest (Wright and Muller-Landau, 2006). Shrub and savanna is divided into tundra and semiarid ecosystem based on a latitudinal distribution where the former is the vegetation type above  $45^\circ\text{N}$  and the latter below this threshold. Grasslands and broadleaf croplands are defined as grass and crop. Finally, non-vegetated land and urban buildup are sparsely vegetated areas (Ahlström et al., 2015).

The grid cell resolution of the satellite data is regridded from  $0.5^\circ \times 0.5^\circ$  to the resolution of each individual model. Since it is a two-dimensional (longitude, latitude) grid, the bilinear interpolation (repeated linear interpolation) method is used.

**Table 1:** Data

<i>i) CMIP6 data</i>			
Model Source-ID/ <i>Institution</i>	Spatial resolution (lat × lon)	Atmosphere/ Land model	Data acquirement
ACCESS-CSM2 ( <i>CSIRO-ARCCSS Commonwealth Scientific and Industrial Research Organisation</i> )	1.2500° × 1.8750°	MetUM-HadGE3-GA7.1 CABLE2.5	Dix et al. (2019), accessed Dec. 2019 (1970-2015); Mar. 2021 (1950-1960), Jan. 2020 (tas 2010-2015), Dix et al. (2019), accessed Dec. 2019 (huss, pr, tas) Feb. 2020 (ps 2015-2095+2095-2100)
BCC-CSM2-MR ( <i>BCC; Beijing Climate Center</i> )	1.1250° × 1.1250°	BCC_AGCM3_MR BCC_AVIM2	Wu et al. (2018b), accessed April 2019 Xin et al. (2019), accessed Mar. 2019
CMCC-CM2-RS5 ( <i>CMCC; Fondazione Centro Euro-Mediterraneo sui Cambiamenti Climatici</i> )	0.9675° × 1.2500°	CAM5.3 CLM4.5 (BGC mode)	Lovato and Peano (2020a), accessed May 2020 Lovato and Peano (2020b), accessed June 2020
CMCC-ESM2 ( <i>CMCC</i> )	0.9675° × 1.2500°	CAM5.3 CLM4.5 (BGC mode)	Lovato et al. (2021a) accessed Dec. 2020 Lovato et al. (2021b), accessed Jan. 2021
EC-Earth3 ( <i>EC-Earth-Consortium</i> )	0.7031° × 0.7031°	IFS cy36r4 HTESSEL	EC-Earth Consortium (EC-Earth) (2019a,b), accessed Mar. 2020
GFDL-ESM4 ( <i>NOAA-GFDL; National Oceanic and Atmospheric Administration</i> )	1.0000° × 1.2500°	GFDL-AM4.1 GFDL-LM4.1	Krasting et al. (2018), accessed Dec 2019 (huss, pr, tas); Aug 2019 (ps) John et al. (2018), accessed June 2019
<i>ii) satellite data</i>			
MODIS ( <i>Moderate-resolution Imaging Spectroradiometer</i> )	0.5000° × 0.5000	MCD12C1 LAI based classification	Friedl and Sulla-Menashe (2015), accessed May 20, 2022
<i>iii) In situ data</i>			
Location	temporal coverage	#stations	
China	1960 - 2010	604	Dou et al. (2021)
USA	2015 - 2017	25	Ritter et al. (2019)
Mexico	2011 - 2016	1	Aguirre-Gutiérrez et al. (2019)

Additionally, observation data of annual dew fall is included to evaluate the modeled data of dew formation. The stations are spread over China (Dou et al., 2021) and North America (Ritter et al., 2019; Aguirre-Gutiérrez et al., 2019). The locations are shown in Fig. 2. The point measurements are given in dew days per a certain time interval. Temporal coverage ranges from three years (Ritter et al., 2019) to 51 years (Dou et al., 2021), shown in Tab. 1 *iii*. The studies are based on meteorological data (Ritter et al., 2019), including field observations (Dou et al., 2021) or microlysimeter and Eddy Covariance Tower measurements (Aguirre-Gutiérrez et al., 2019).

## 2.2 Methods

In this section, the method of calculating dew point temperature is shown first. Second, the definition of a dew day in this study is shown. Next, the validation and correction of the data is explained. Last, post-processing of the data is shown.

### 2.2.1 Dew point temperature

Dew frequency depends on surface temperature ( $T_s$ , in K) and dew point temperature ( $T_d$ , in K), which depends on the relative or specific humidity (RH in % or  $q$  in  $\text{g kg}^{-1}$ ) and the surface pressure ( $p_s$  in Pa).

In order to calculate dew point temperature ( $T_d$ ), the vapor pressure ( $e$  in Pa) and saturation vapor pressure ( $e_s$  in Pa) are needed. According to Monteith and Unsworth (2013) - Eq. 2.3 - the vapor pressure ( $e$ ) is defined as follows:

$$e = \frac{qp}{\varepsilon} \quad , \quad (1)$$

where  $\varepsilon$  is the ratio of the mass fraction of water vapor ( $m_{vw} = 18 \text{ g mol}^{-1}$ ) to the average mass fraction of the air ( $m_{air} = 29 \text{ g mol}^{-1}$ );  $\varepsilon = m_{vw} / m_{air} = 0.62$ .

The saturation vapor pressure ( $e_s$ ) is calculated using the Equation 2.7 of Monteith and Unsworth (2013).

$$e_s(T) = e_s(T^*) \exp\left(\frac{A(T - T^*)}{(T - T')}\right) \quad . \quad (2)$$

Within the temperature range of  $0^\circ\text{C}$  to  $35^\circ\text{C}$  the following approximation can be done:

$T^*$  is 273 K,  $T' = 36 \text{ K}$  and  $A = 17.27$ .  $e_s(T^*)$  then is equal to  $e_s(273 \text{ K}) = 0.611 \text{ kPa}$ . This empirical approximation is known as the Tetens equation and can be written as follows (Tetens, 1930):

$$e_s(T) = 0.611 \text{ kPa} \exp\left(\frac{17.27(T - 273 \text{ K})}{(T - 36 \text{ K})}\right) \quad . \quad (3)$$

The dew point temperature is reached when  $e = e_s(T_d)$ . Rearranging the Equation 3,  $T_d$  can be estimated which is shown in the following equation (Monteith and Unsworth (2013); Eq. 2.29).

$$T_d = \frac{T' \times \ln\left(\frac{e}{e_s(T^*)}\right) - (A \times T^*)}{\ln\left(\frac{e}{e_s(T^*)}\right) - A} \quad . \quad (4)$$

Again, using the empirical values defined by Tetens (mentioned above), the result is given in degrees Kelvin. The equation can be written as follows:

$$T_d = \frac{36 \text{ K} \ln\left(\frac{e}{0.611 \text{ Pa}}\right) - (17.27 \times 273 \text{ K})}{\ln\left(\frac{e}{0.611 \text{ Pa}}\right) - 17.27} \quad . \quad (5)$$



Relative humidity (RH) is given as the ratio of vapor pressure to saturation vapor pressure (Monteith and Unsworth, 2013) and expressed in percent (%):

$$RH = \frac{e}{e_s(T)} \times 100 \text{ (\%)} . \quad (6)$$

### 2.2.2 Definition of the number of dew days

In this master's thesis, the number of dew days is estimated based on favorable atmospheric conditions, as there is no variable available indicative for dew formation, as mentioned in Section 2.1.1. Even though multiple atmospheric states are favorable for dew formation according to empirical studies (see Section 1.1), only  $T_s \leq T_d$  is included in the thesis. Due to the lack of a saved variable indicative for  $T_s$ , air surface temperature *tas* is used instead. The conditions are therefore tested on  $tas \leq T_d$ .

Time steps with temperatures below 0°C are not considered as favorable condition even when  $tas \leq T_d$  is fulfilled since this is a limit of Equation 5. In other words, when temperatures are below the freezing point ( $T < 0^\circ\text{C}$ ), frost instead of dew is more probable to form. Therefore, time steps with temperatures below zero degrees Celsius are not tested whether the conditions are fulfilled or not.

Also, wind is not considered, since it influences dew formation on a local-scale. This effect is not properly represented in the models with the given grid resolution. Therefore, the effect of wind on dew formation is neglected in this study.

Favorable days for dew formation are defined by testing the data on the temperature condition. When the air temperature (*tas*) is equal to or drops below the calculated dew point temperature ( $T_d$ ) once a day, the day is counted as a dew day.

$$tas \leq T_d$$

This is shown in Figure 1a, in the lower panel *tas* (blue) and  $T_d$  (orange). The top panel shows if  $tas \leq T_d$  is true (yes) or false (no) in three hourly (gray) and daily (black) resolution.

Hours with precipitation are not considered since the atmosphere is saturated when it rains; most rainy days would be seen as dew days. The goal of the thesis is to estimate the change in dew days, so time steps with precipitation are excluded even when the set condition (shown below) is fulfilled. In other words, the day is counted as dew day when there is no precipitation and when  $tas \leq T_d$  is fulfilled at least once a day (shown in Fig. 1b additional to *a* three hourly time-periods without precipitation are shown in the top panel of *b* (green)). We define dew days as the days when the following conditions

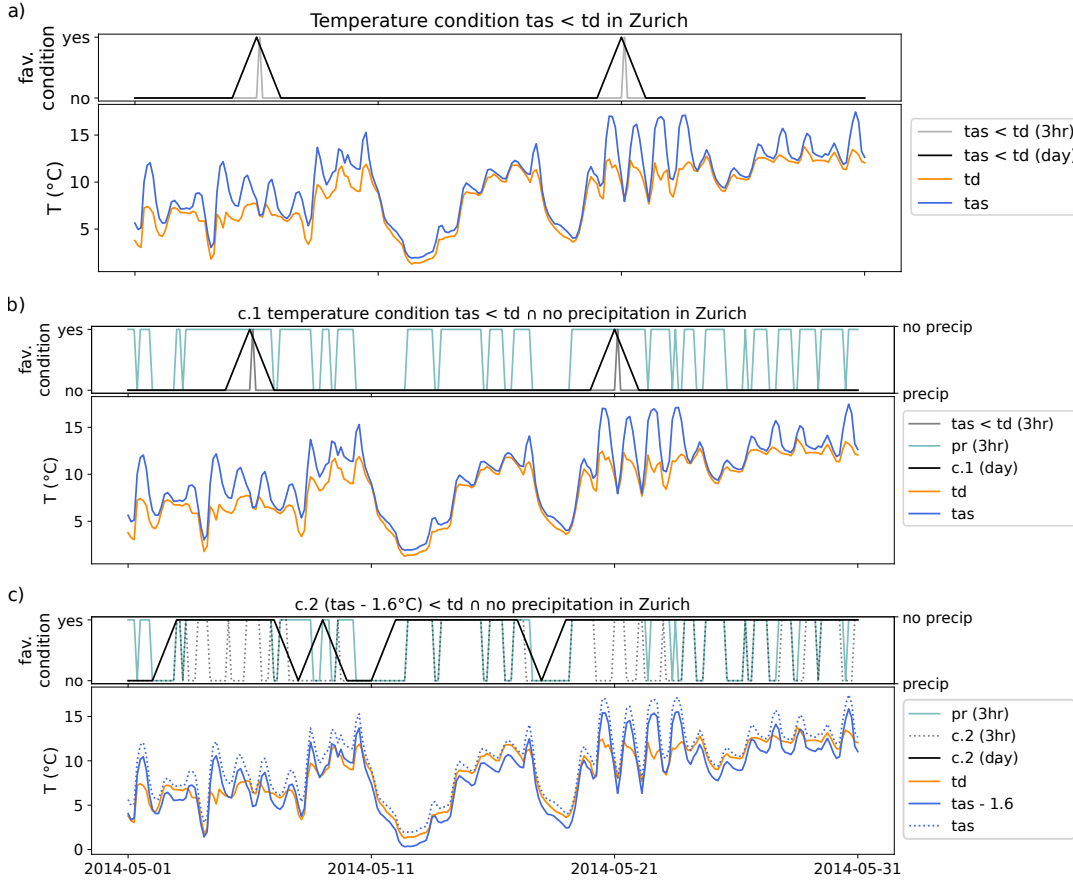


**Figure 1:** Example of conditions with air surface temperature ( $tas$ ) in blue and dew point temperature ( $td$ ) in orange in Zürich in May, 2014. In a) a day is counted as dew day when  $tas \leq T_d$  (top panel) in black and three-hourly resolution in gray. b) when a) is fulfilled, and the condition excludes precipitation days (in b top panel in green (condition c.1)). c) shows condition  $tas - \alpha \leq T_d$  with  $\alpha = 1.6^\circ\text{C}$  (condition c.2).

are fulfilled:

$$tas \leq T_d \quad \cap \quad \text{no precipitation} \quad (\text{c.1})$$

This condition (c.1) is referred to as  $tas \leq T_d$ .

In this master's thesis, precipitation is defined as values above  $10^{-4} \text{ kg m}^{-2} \text{ s}^{-1}$  ( $0.36 \text{ mm h}^{-1}$ ). The threshold for precipitation was determined by comparing modeled precipitation days to meteorological data (Aguirre-Gutiérrez et al., 2019; meteoblue AG, n.d.). The global pattern is similar to Douville et al. (2021).

Since the modeled temperature is based on a temperature at a height of two meters above the roughness level, it might be more difficult to meet the temperature condition there than at the surface. In addition, dew point temperature is faster reached at the surface, since by night, skin surface temperature drops faster than air surface temperature. Favorable days for dew formation are not perfectly represented by fulfilling the atmospheric conditions of  $tas \leq T_d$ . In fact, air surface temperature is not an ideal approximation for skin surface temperature. By testing additional conditions, we can find

the best suited approach to represent an estimation of dew days within the given limitations.

Indeed, a comparison between the modeled data to observation studies showed that by slightly adjusting  $tas$ , a better representation of estimated dew days can be achieved. Therefore, a less stringent temperature condition is applied than in the former condition (c.1). Instead of  $tas \leq T_d$  the temperature condition is set to  $tas - \alpha \leq T_d$  so that the air temperature reaches the dew point temperature faster.  $\alpha$  are values between 0.2°C to 5.0°C. Figure 1c shows an example with  $\alpha = 1.6^\circ\text{C}$ . The evaluation of the best suited  $\alpha$  is statistically evaluated which is described in Section 2.2.3.

Additionally, the correction of  $tas$  covers atmospheric conditions with relative humidity below 100%. As mentioned above, the probability of dew formation starts to increase when relative humidity at two meter height is above 73% (Aguirre-Gutiérrez et al., 2019). It is possible that dew can form even when  $tas$  is slightly larger than  $T_d$ .

This condition also excludes time steps with precipitation for reasons mentioned above (Fig 1c). It can be summarized as:

$$tas - \alpha \leq T_d \quad \cap \quad \text{no precipitation} \quad (\text{c.2})$$

It will be referred to as  $tas - \alpha \leq T_d$  from now on.

The above defined conditions (c.1 and c.2) are only tested on time steps when temperatures are above or equal to zero degrees Celsius, and there is no rain. The number of days that are tested on the condition (c.2) is later referred to as the *number of counted days*. The number of counted days increases with time due to climate change. This affects also the estimated dew days. With an increasing number of counted days, more days are tested if the condition is fulfilled. Therefore, estimated dew days can simply increase due to more opportunities. To negate this effect, the estimated dew days can be calculated relative to counted days. This ratio shows whether the change in dew days with time is because of a changing number of counted days or due to a change in atmospheric conditions. In other words, when the ratio of estimated dew days relative to counted days shows an increase, we can assume that the rise in dew days is due to changing atmospheric conditions.

### 2.2.3 Evaluation and bias-correction

In order to evaluate the estimated dew frequency, historical model data from 1980 to 2010 is compared to observational data on dew frequency from different studies (Ritter et al., 2019; Dou et al., 2021; Aguirre-Gutiérrez et al., 2019). All studies together count 628 stationary data points all of which

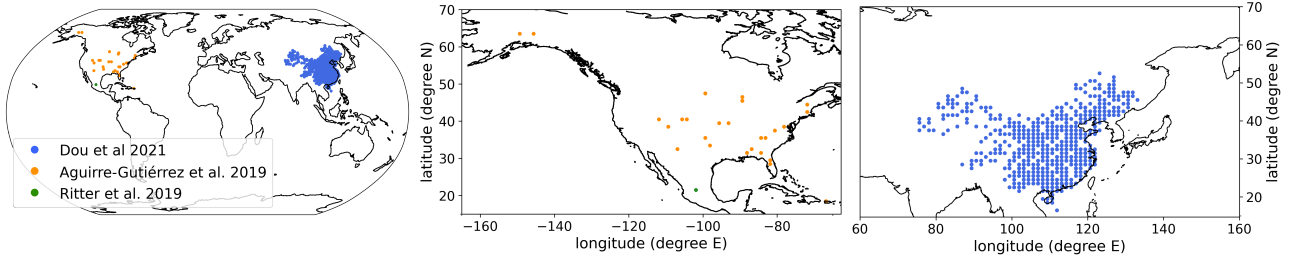


**Figure 2:** The locations of the stationary data points from the different studies, whereas blue represents (Dou et al., 2021), green (Aguirre-Gutiérrez et al., 2019), and orange (Ritter et al., 2019).

provide the annual number of dew days. The locations of the stations are shown in Fig. 2.

Since annual observations do not overlap exactly with modeled data results of estimated dew days, and the different studies do not provide the same temporal coverage, the annual mean of the model output is compared to the corresponding annual mean of the observation of the specific grid cell. Note that the observation data is at a particular location, but the model represents this location using a mean of an area represented as grid cell. The resolution of the models is shown in Tab 1 *i*. When two or more meteorological stations are represented in one grid cell, the mean of dew days across the stations is considered when comparing it with the modeled dew days. This helps to obtain more robust results.

### *Statistical methods and the evaluation of the condition*

In order to test and quantify the agreement of the modeled condition with the observations, various statistical analyses are applied, such as the linear regression, Spearman correlation, correction based on ordinary least squares correction (see Fig. 3 and 4; all conditions are shown in the Section 7, Supplementary Figure 1), and a Kolmogorov-Smirnov test. The statistical methods are discussed in the following sections.

First, to test the relation between observation and the modeled data, a linear least-square regression analysis is performed, using the modeled results of each defined condition in relation to the observation data. By computing the regression line, the best linear fit between the variables is estimated.

However, even with a well fitting line, the data may have a systematic error. This is the bias and is calculated by the difference from the mean of the observation to the mean of the modeled data points ( $bias = \overline{observation} - \overline{model} = \bar{y} - \bar{x}$ ). It is an indicator of the offset from the observation to the modeled data. In other words, the variables are linearly dependent, but there is a systematic deviation from the modeled data to the observation, which is shown in a highly positive or highly negative bias.

Besides the linear regression, the *Spearman correlation coefficient* ( $\rho$ ) is computed to measure the interdependence of the modeled data to the observations. A non parametric correlation coefficient

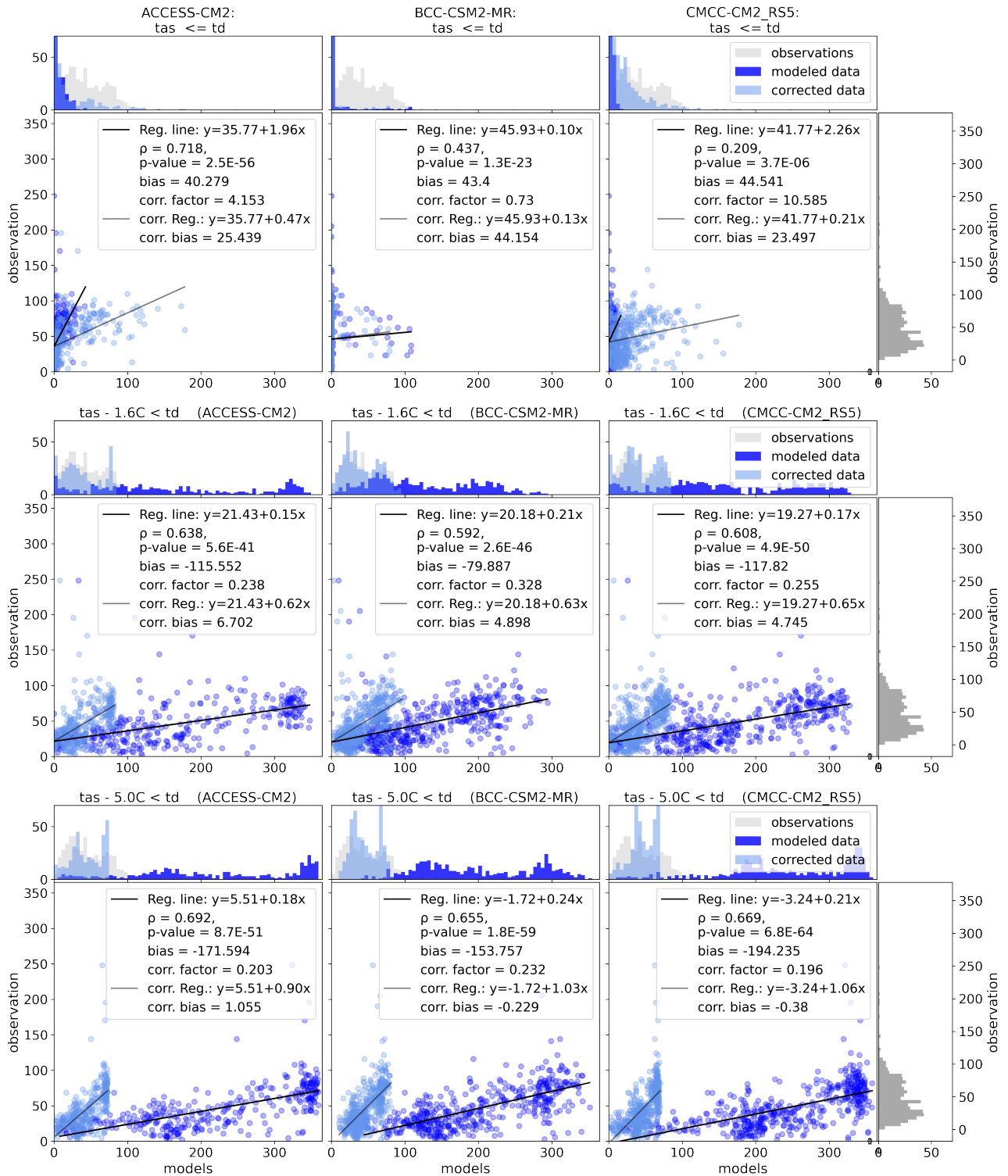


**Figure 3:** Scatterplot and statistical analysis of the models (x-axis) and observations (y-axis) including the histogram. For  $\alpha = 0.0, 1.6, 5.0$  from top to bottom. Modeled data are shown in blue, data after the bias-correction in light blue, and observations in gray. The following models are shown from left to right: ACCESS-CM2, BCC-CSM2-MR, and CMCC-CM2-RS5.

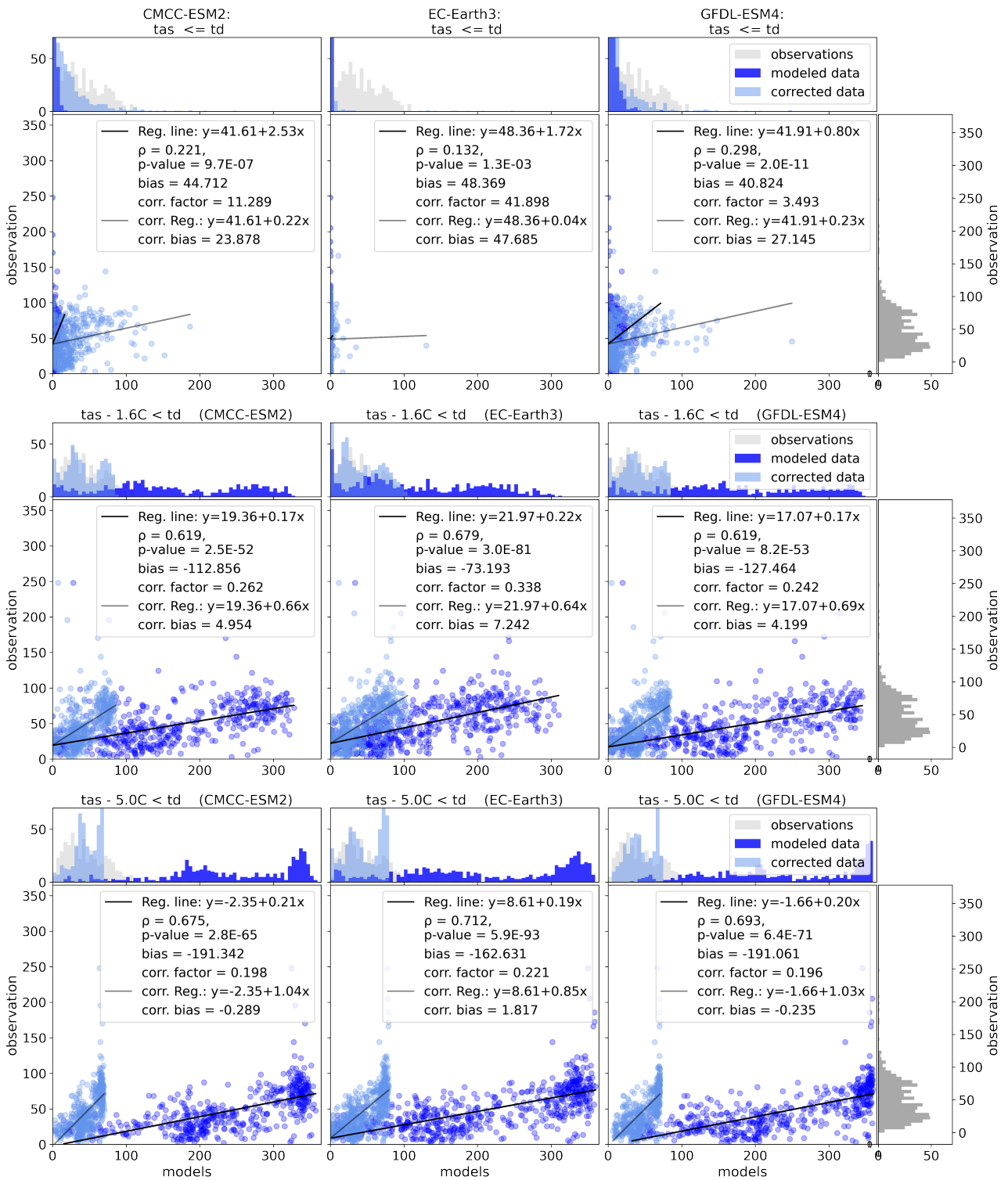


**Figure 4:** Scatterplot and statistical analysis of the models (x-axis) and observations (y-axis) including the histogram. For  $\alpha = 0.0, 1.6, 5.0$  from top to bottom. Modeled data are shown in blue, data after the bias-correction in light blue, and observations in gray. The following models are shown from left to right: CMCC-ESM2, EC-Earth3, and GFDL-ESM4.

method is used, since the data is not normally distributed.  $\rho$  is a value between -1 to 1, with negative values for a negative correlation and positive values for a positive correlation. The significance level is expressed as p-values (here  $p - value < 0.05$ ). To have a robust condition,  $\rho$  is supposed to be strong with a small bias.

The Kolmogorov-Smirnov test (KS) quantifies the offset of the cumulative density function of two distributions. The KS statistics indicates if the tested two variables show an equal distribution. When the value is small, it means that the two variables have a similar distribution. An additional low significance level shows that the variables are not from the same distribution. In other words, if the distribution of two data sets overlap but have different origin, KS is small and not significant.

The Spearman correlation ( $\rho$ ) of the modeled data to the observation data can be strengthened with the correction of  $tas$  (Fig 3 and 4). The correction is done by subtracting a factor  $\alpha$  of  $tas$  (c.2:  $tas - \alpha \leq T_d$ , shown in Section 2.2.2).  $\rho$  ranges from 0.1 without correction of  $tas$  and up to 0.7 when  $tas$  is corrected by  $\alpha = 5.0$ . It varies only slightly among models regarding a given  $\alpha$ .

On the other hand, the bias is negatively affected by the correction of  $tas$ . It decreases from around 50 to -200. This implies that the offset between modeled data and observations increases due to higher correction, even though the correlation strengthens. Additionally, the distribution of the modeled values poorly overlaps with the observation's distribution (Fig. 3 and 4). Moreover, the overlap worsens with a higher correction of  $tas$ . The higher  $\alpha$  is, the more spread out is the modeled data.

### ***Bias-correction***

In order to achieve better results, the bias is further corrected by multiplying the modeled data with a factor  $\beta$  as follows:

$$\widehat{\text{dew days}}_{\text{bias-corrected}} = \text{dew days} \times \beta \quad (6)$$

The correction is based on the ordinary least-square method with which a factor  $\beta$  is estimated for each condition.  $\beta$  can correct the bias and, therefore, the distribution to become closer to the observation values. The bias-correction factor ( $\beta$ ) for each condition is shown in Fig. 3 and 4.

By applying the bias-correction (Eq. 6) on the data, the bias is further reduced. Figure 5b illustrates the improvement of the correction on the bias from non bias-corrected (shaded colors) to bias-corrected data. With increasing  $\alpha$ , the corrected bias is decreasing, and the offset to the observation data decreases. Moreover, bias-correction leads to a better fit between the distribution of the modeled data and observation for all models (Fig 5c).

Although  $\alpha = 5.0$  is the best fit considering  $\rho$  and the corrected bias (Fig. 5a and b), the corrected distribution of the model fits the distribution of the observation poorly (Fig 5c). The Kolmogorov-

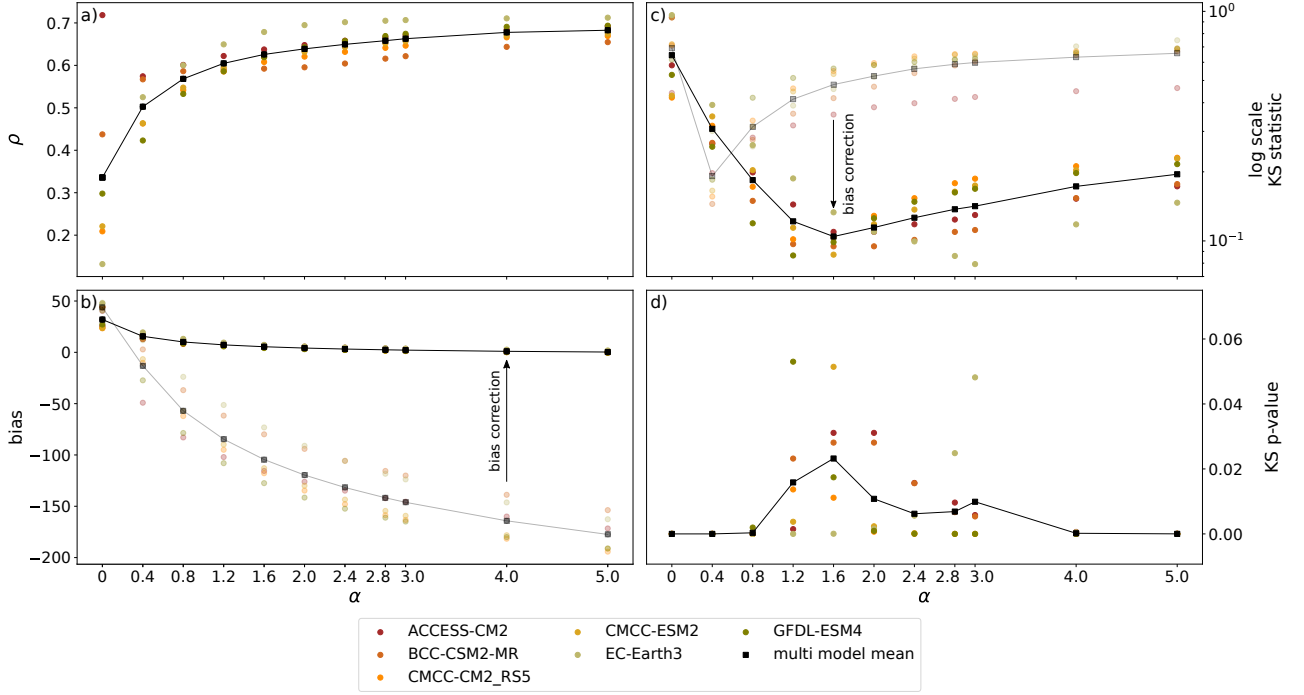


**Figure 5:** Relationship of  $\alpha$  ( $tas - \alpha \leq T_d$ ) for the different condition (x-axis) to a) the Spearman correlation coefficient ( $\rho$ ), b) the bias before correction (shaded) and after correction, c) Kolmogorov-Smirnov test with logarithmic scale before bias-correction (shaded) and after bias-correction, and d) the p-value of Kolmogorov-Smirnov test after bias-correction. The multi-model mean is shown as black squares, and the models are differently colored dots.

Smirnov test reveals the condition  $tas - \alpha \leq T_d$  after bias-correction as best fitting distribution, with KS statistic in average around 0.1 with a non significance level ( $p - value > 0.02$ ). The high p-value indicates the different origin of the modeled and observational data.

In summary, the different statistical methods revealed that  $\alpha = 1.6$  ( $tas - 1.6^\circ\text{C} \leq T_d$ ) best represents the observations after bias-correction.  $tas$  correction of  $\alpha = 1.6$  has a high correlation coefficient  $\rho$  across all models. Additionally, the bias after the bias-correction is between 4.5 to 7.5, and KS test indicates this condition as the best fitting distribution. The condition  $tas - 1.6^\circ\text{C} \leq T_d$  is used for further calculations of the favorable conditions for dew days.

### 2.2.4 Post-processing

Before analysing the data, it has been post-processed as follows.

#### *Weights*

To properly calculate a mean over a certain area on a globe, the grid cell must be weighted according to its size, since the area of a grid cell is shrinking with increasing latitudinal degrees. Additionally, the land fraction must be taken into account because in coastal areas the grid cell includes water which results in a lower area where dew can form. The data is weighted accordingly. Usually, the variables



are provided as `sftlf` for land fraction and `areacella` for cell area (references according to model output Tab. 1).

Since there is no model output of BCC-CSM2-MR, which would provide the variable for weighting (`areacella` and `sftlf`), it must be additionally calculated. The land fraction is determined by the variable `ra` which is indicative for Land Carbon Mass flux by plant respiration (Wu et al., 2018a). Next, the area per cell is calculated according to the following equation:

$$\text{areacella} = \frac{\cos(\text{lat})}{\sum \cos(\text{lat})} \cdot \frac{A_{tot}}{\text{longitudinal resolution}} \quad (7)$$

The total surface area ( $A_{tot}$ ) of the Earth ( $5.1009 \cdot 10^{14} \text{ m}^2$ ) is calculated by the mean of the total surface area of the models ACCESS-CM2, CMCC-CM2-RS5, CMCC-ESM2, and GFDL-ESM4.

### *Multi-model mean*

As already mentioned, models within CMIP6 are based on a similar framework so that a multi-model mean can be done to provide more robust outcomes.

In order to calculate the multi-model mean, the models are regridded to the same spatial resolution with a bilinear interpolation method, since it is a two-dimensional grid. In this case, the new grid cell resolution is set to  $1.2500^\circ \times 1.8750^\circ$  (lat  $\times$  lon), according to the lowest spatial resolution of the six models (ACCESS-CM2). After regridding all models, a mean of the models is calculated for each grid cell and time step.

## 3 Results and Discussion

This section shows and discusses the results of the analyzed data. First, the climatology of dew days is exposed. Then the global change in favorable conditions for dew days is presented by global trends and global patterns. The latter case considers the model differences and the changes relative to countable days. The second part discusses changes in the estimated number of dew days in the zonal mean and the different biomes. Last, the seasonal changes in the Amazon are analyzed in more detail.

### 3.1 Climatology of estimated number of dew days

The estimated dew days occurrence differs globally (Fig. 6). A distinctive pattern can be seen, which is noticeably similar to global temperature and humidity (IPCC, 2021; Byrne and O’Gorman, 2013). On the one hand, dew mostly occurs in the Tropics due to the high temperatures and relative humidity. On the other hand, dew frequency is low in warm and dry areas, such as the Middle East,

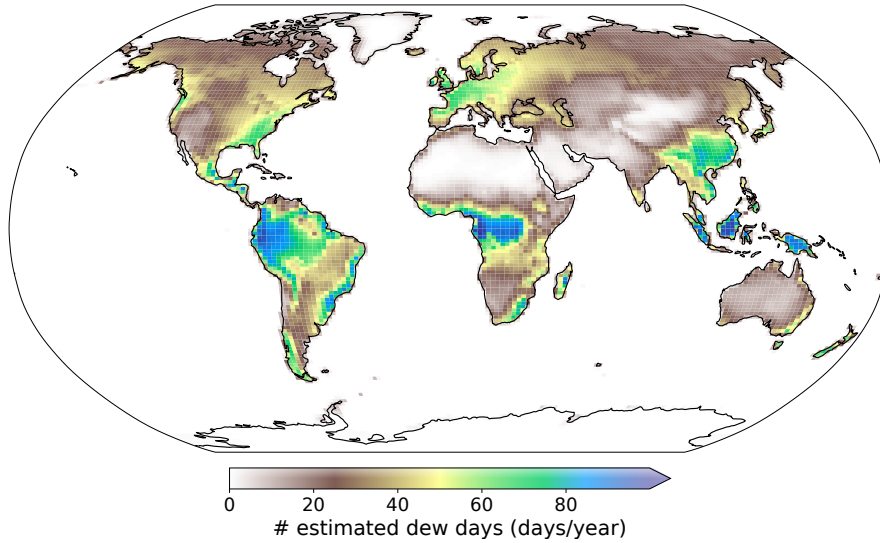


**Figure 6:** The multi-model mean of the global dew occurrence in 1950-1980.

North Africa, and Australia. Even though in the previously mentioned areas, the amplitude of the diurnal temperature range is large (Lindvall and Svensson, 2015), the amount of water vapor seems to be too small to reach dew point temperature at night. This indicates that relative humidity plays an important role in dew formation in warm areas.

An intermediate to low number (e.g., 10 - 60 dew days per year) of estimated dew days occurs in temperate zones (Fig. 6). Besides temperature and relative humidity, dew occurrence depends on the number of counted days in this area. An example is the Eurasian mid-latitudes, where the westerlies influence the weather. The winds bring humid air to the continent, which is favorable for dew to form. Nevertheless, the further inland, the dryer air gets, and dew occurrence decreases with distance to the ocean. North Europe shows less estimated dew frequency since there are more days with temperatures below  $0^{\circ}\text{C}$  and, therefore, fewer dew opportunities.

A low estimated number of dew days is also noticeable in the northern high latitudes (Fig. 6). The estimated number in this area is controlled by the counted days. Temperatures are more often below  $0^{\circ}\text{C}$  than in lower latitudes. In other words, dew frequency is lower due to fewer opportunities for dew to form.

The climate influences the biomes, where land and atmosphere constantly exchanging water. In general, temperature influences the water vapor-pressure deficit ( $\text{VPD} = e_s - e$ ) in the atmosphere. VPD increases with higher temperatures; this induces a higher evapotranspiration rate (Dai et al., 2018). Besides temperature, vegetation cover can also influence the evapotranspiration rate (Wang et al., 2018; Zha et al., 2010). The higher the vegetation cover fraction, the higher the evapotranspiration (Wang et al., 2018). Evapotranspiration, or rather VPD, influences favorable conditions for dew forma-

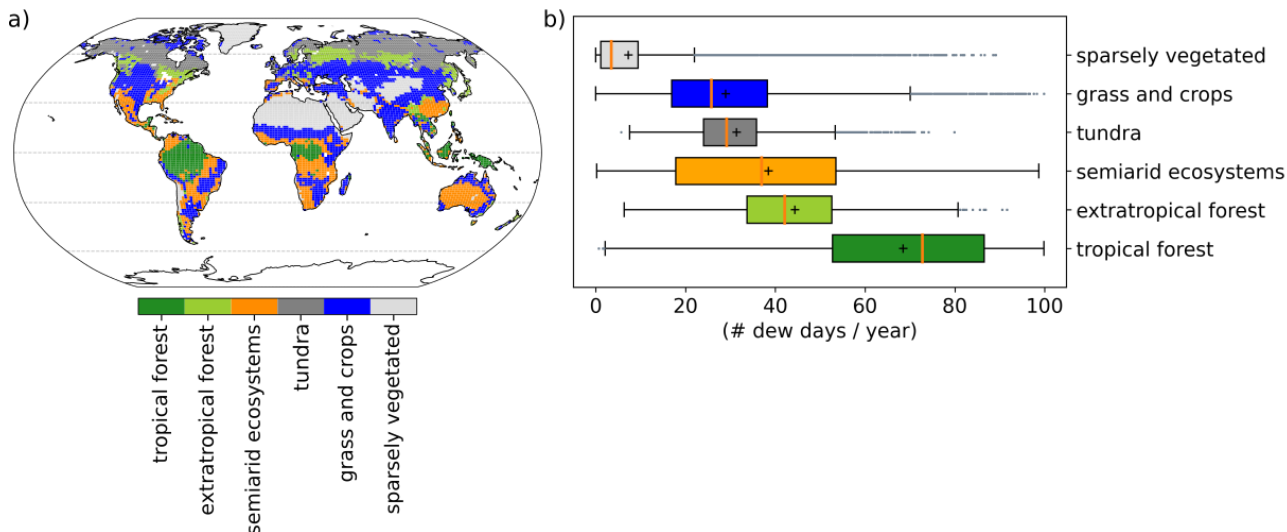


**Figure 7:** The multi-model mean of a) the global map of the biomes based on MODIS data (Tab.1*i*) and b) the weighted distribution of estimated dew days regarding biomes as annual average in 1950-1980.

tion. The evapotranspiration based on vegetation cover seems to be similar to our results (Fig.7a,b). The conditions for increased evapotranspiration rates favor dew formation with low VPD, i.e., high relative humidity.

Figure 7b shows the estimated dew frequency for the different biomes. The discussed biomes are based on the MODIS data (Section 2.1.2) and do not fully coincide with the modeled land cover but reflect the actual land cover found today. The figure illustrates that high-density vegetation covers, such as tropical forests, show a high estimated dew frequency. On average, there are 70 days per year favorable for dew formation. Depending on the location, the number of dew days varies between 0 to 100. Grass and crops, tundra, semiarid ecosystems, and extratropical forests show close results in estimated dew days. The differences between the biomes of grass and crops and extratropical forests may be explained by agricultural farming. After crop yield, dew fall events drop dramatically (Xiao et al., 2009).

As mentioned above, extratropical forests show more similar dew frequencies to grass and crop land and tundra rather than to tropical forests. This is mainly due to the temperature differences between extratropical and tropical forests but may also be partly explained by the vegetation type. Extratropical forests include deciduous forests as well as evergreen vegetation, where the latter has lower evapotranspiration rates than deciduous forests in a subhumid region or grassland in a semiarid region (Zha et al., 2010). This difference between the two evapotranspiration rates of one biome decreases the total evapotranspiration over some areas of extratropical forests during summer compared to tropical forests.

The evapotranspiration rate might not fully explain the difference in estimated dew days between

extratropical and tropical forests. However, evapotranspiration might be a more important driver in water-limited areas than in non-water-limited areas in the mid-latitudes. Therefore, vegetation-driven evapotranspiration rates might be less important in extratropical forests than in tropical forests during the dry season.

Besides evapotranspiration, a large seasonal temperature change influences northern areas covered in extratropical forests, grass and cropland, or tundra, unlike tropical forests. The low winter temperatures in the northern areas decrease the counted days and, therefore, the possible number of dew days (Section 2.2.2).

In summary, dew highly depends on the climate associated with temperatures and relative humidity. Besides the given climate, other factors, such as vegetation cover, additionally influence favorable conditions for dew formation. A high fraction of land cover may positively affect the estimated number of dew days. All in all, climate and vegetation cover may influence the favorable conditions for dew formation.

Overall, our results in estimated dew frequency coincide with the study of Vuollekoski et al. (2015), one of the few studies which model dew frequency based on climate data on a global scale. For the multi-model mean, the global results are underestimated for the period 1979-2012 in comparison to Vuollekoski et al. (2015) (shown in Fig. 8 for the summer months). However, Vuollekoski et al. (2015) model the potential dew on artificial surfaces optimized for dew to form. Hence, dew can be expected more frequently than on natural surfaces. Additionally, less seasonal variability is shown by Vuollekoski et al. (2015) compared to this study. The differences could be based on the validation data. The physical characteristics for dew formation that apply to a certain region do not always apply everywhere (Yu et al., 2020). Although the mean of the estimated dew frequency differs be-

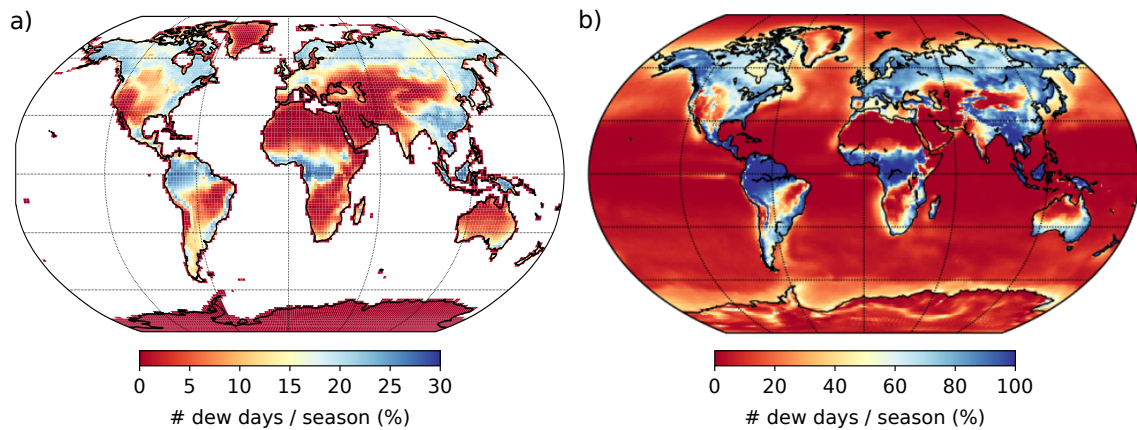


**Figure 8:** a) Seasonal mean of dew frequency from 1979-2012 (June, July and August 'JJA') in comparison to b) Vuollekoski et al. (2015) dew frequency on artificial surfaces (Figure retrieved from Vuollekoski et al. (2015); Fig 4). Note that the color axis differs.

tween Vuollekoski et al. (2015) and this study, the spatial pattern is consistent. Altogether it can be concluded that the results of the estimated dew days are within a reasonable range.

## 3.2 Global change in estimated dew days

First, the global trend of estimated dew days is shown. As the global trend is a summary of the regional trends, we next discuss the global pattern of change. This is initially divided into two sections, with model robustness being discussed first. The detection of robust areas helps to assess the results of further analysis. The last subsection looks at global patterns and how they change from different perspectives.

### 3.2.1 Global trend in estimated dew days

The global mean of the estimated number of dew days is analyzed using the models' time series and the multi-model mean. The results show a globally increasing trend in the estimated number of dew days per year. For the period 1950 - 2100, the weighted global mean is depicted in Fig. 9 where panel a) shows the absolute number and panels b) - f) show their relative values.

The global multi-model mean shows a slight increase in dew days per year of about 4 days from 1950 to 2100 (Fig. 9a and b). Almost all models agree on the globally increasing trend except ACCESS-CM2, which indicates a decrease of 2%. However, when the change is relative to the number of counted days in a year, three out of six models show a global decrease in dew days, whereas the multi-model mean has no major change with time (Fig. 9c).

The shift from an increasing to a decreasing trend (Fig 9b to c) is the result of the growing number of counted days (Fig. 9d). In other words, the increase in estimated dew days for the two models (BCC-CSM2-MR, GFDL-ESM4) mainly occurs due to more days at which dew can form, whereas the other models keep the trend, even though the number of countable days increases. It indicates an increase of dew days regardless of the number of counted days for the models but BCC-CSM2-MR and GFDL-ESM4.

When only the number of counted days is considered, a clear upward tendency across all models is noticeable (illustrated in Fig. 9d). The multi-model mean shows a rise of around 5%. The temperature has a higher influence than days without precipitation (Fig 9e and f); mainly because temperature increases globally, whereas precipitation has a second-order change with increasing temperatures (Douville et al., 2021).

Even though the temperature increases globally (IPCC, 2021), mid- to high latitudes are most affected

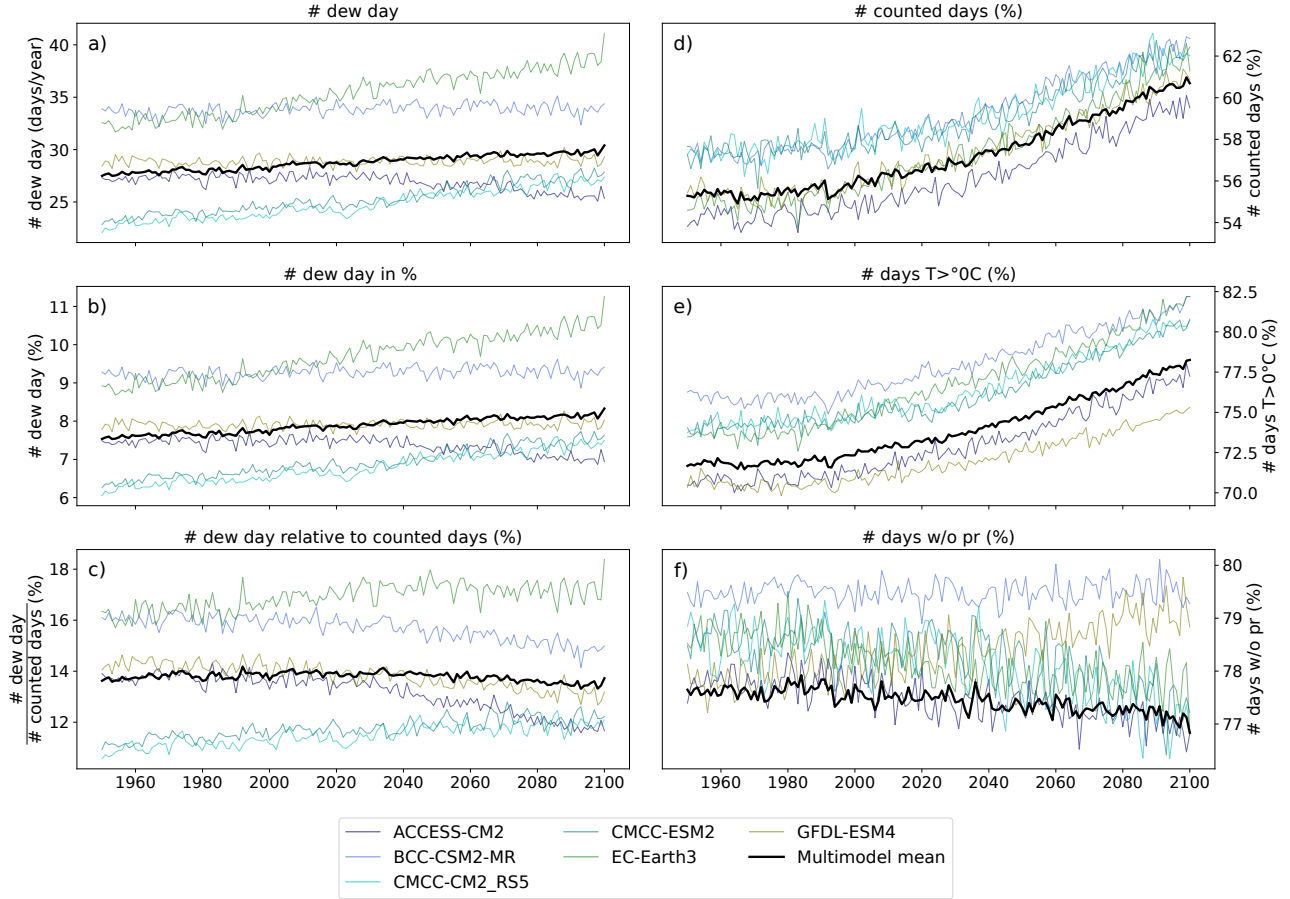


**Figure 9:** Weighted global mean of the number of days favorable for dew formation per year from 1950 - 2100. The Figure shows a) the absolute annual number of estimated dew days, b) the relative number of dew days, c) the number of dew days relative to counted days, d) the number of counted days, e) days with temperatures above  $0^{\circ}\text{C}$ , and f) days without precipitation. The panels d) - f) are shown as relative changes.

by the increasing number of days with temperatures above  $0^{\circ}\text{C}$  (not shown). Nowadays, temperatures in these climate zones are often below freezing point. With a warmer climate, this number will decrease. With the increase in days with temperatures above  $0^{\circ}\text{C}$ , there are more countable days and, hence, more possibilities for dew to form. Indeed, Fig.10 indicates that these areas show a high increase in dew days. The possible increase in dew might be based on the framing of the condition (Eq. 5). With Equation 5, temperature conditions below freezing point are excluded and, therefore, do not fulfill the condition for dew formation of this master's thesis. However, dew may still be present but in the form of frost. So with warming temperatures, frost days may decrease in favor of dew days. In the multi-model mean, slightly fewer days without precipitation are expected with time (Fig 9f). This coincides with Lee et al. (2021). The trend in this master thesis is less pronounced since the days without rain are counted instead of quantifying precipitation. This herein sets a threshold for precipitation based on meteorological data (see Section 2.2.2). This may be less sensitive in detecting precipitation changes since values below the threshold are not considered. However, there is no need to quantify precipitation changes regarding the counted days.

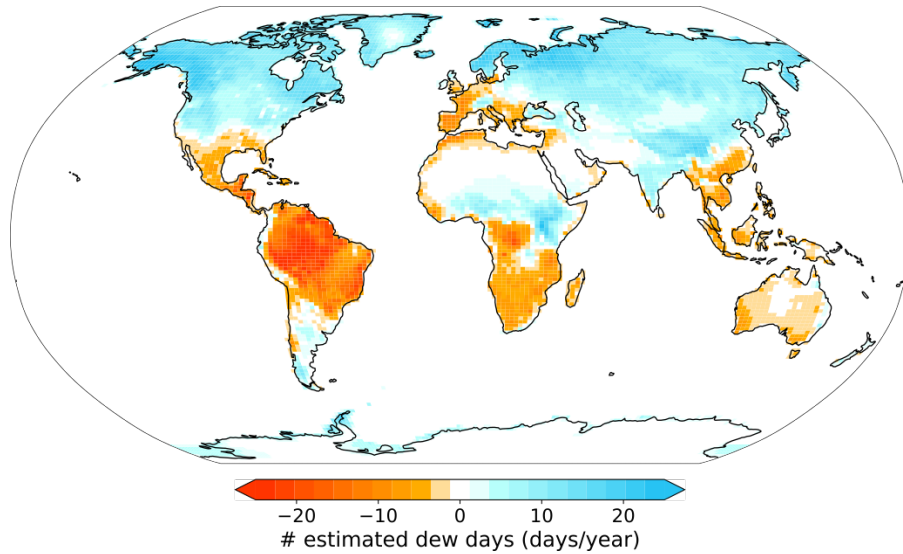


**Figure 10:** The multi-model mean of the estimated change in dew days from 1950-1980 to 2070-2100.

There is a disagreement in the trend in days without precipitation among models. Besides the spatially different tendencies in non-rainy days, the challenging dynamics of the water cycle change influence the modeled results. There are regions with intermediate certainty of changes in precipitation (Douville et al., 2021).

Besides the clear increase in dew days above  $45^{\circ}\text{N}$ , there are spatially different trends (Fig. 10). It is noticeable that the Southern Hemisphere is dominated by a decrease in estimated dew days, whereas the area between the equator and  $45^{\circ}\text{N}$  shows both an increase and decrease in the estimated dew frequency. The deviating regional changes in a model can influence the global trend. In Figure 9a and b, the differences in the trend of the estimated number of dew days are depicted.

Furthermore, in situ studies show different trends in dew frequency (Hao et al., 2012; Dou et al., 2021; Feng et al., 2021). On the one hand, increasing temperatures are disadvantageous for dew formation due to decreasing relative humidity (Dou et al., 2021; Feng and Fu, 2013). On the other hand, the warmer temperature during the day creates a higher amplitude in the diurnal temperature cycle. In warmer conditions, the atmosphere can hold more water vapor (Hao et al., 2012). This helps to reach dew point temperature by night faster and can enhance dew formation.

The measurement of dew is difficult, and the results highly depend on the calibration and definition of dew (Agam and Berliner, 2006). The disagreement not only emphasizes the importance of normalizing the measurement method for dew but also that dew formation and its change depend on the location (Yu et al., 2020).

In summary, although the modeled data show a small increase in the global estimated number of dew days (Fig. 9), there are strong changing trends on a local scale (Fig. 10). The global mean in

the number of counted days increases with time. These days are influenced by both temperature and precipitation in latitudes above 30°N and below 30°S. Between 30°N and 30°S, only precipitation influences the counted days.

### 3.2.2 Global patterns and model differences

The global mean summarizes local changes. To better understand the overall trends, the global pattern is analyzed as change in the annual mean of estimated dew days from the periods 1950-1970 to 2070-2100 (Fig. 11).

In general, the Northern Hemisphere indicates a clear increase in the annual mean of estimated dew days with maxima in the subpolar regions (Fig. 11). A declining number of dew days is mostly located in the Southern Hemisphere with few exceptions, such as the Mediterranean, western and central Europe (except for EC-Earth3), as well as parts of Southeast Asia. However, there are disagreements across the models, for example, in Central and North America and the African Tropics. A strong agreement on the decrease in estimated dew days is shown in the Amazon, in parts of Southeast Asia, and parts of southern Africa.

Three rather prominent patterns are distinguishable across the models regarding the estimated dew days. ACCESS-CM2, BCC-CSM2, and GFDL-ESM4 show a clear decrease in Africa with a slight increase in parts of the Sub Sahara, while in contrast, CMCC-CM2-RS5 and CMCC-ESM2 predict an increase around the Congo Basin, whereas EC-Earth3 does not predict any declining trend in Africa north of the equator except in the coastal areas. Moreover, EC-Earth3 is the only model which expects an increasing trend in central Europe. Further, the trend at the eastern coast of India is divided into a rise in estimated dew days (CMCC-CM2-RS5, CMCC-ESM2, and EC-Earth3) and a decline or a patchy pattern (ACCESS-CM2 and BCC-CSM2-MR or GFDL-ESM4).

CMCC-CM2-RS5 and CMCC-ESM2 were simulated with the same atmospheric model (Tab 1) and, thus, show very similar results. ACCESS-CM2, BCC-CSM2, and GFDL-ESM4 disagree in some areas (e.g., North America or Australia). Nevertheless, the overall pattern matches well. EC-Earth3, however, deviates from the other models in many regions.

The deviation among the models is not only based on the different boundary settings of the used climate models but may also originate partly from biased climate outputs. For instance, in India, ACCESS-CM2 is negatively biased in precipitation (Bi et al., 2020), which could lead to a higher number of countable days, i.e., more possible days for dew to form. Additionally, BCC-CSM2-MR shows a warmer air surface temperature in comparison to ERA-Interim reanalysis (Wu et al., 2019),



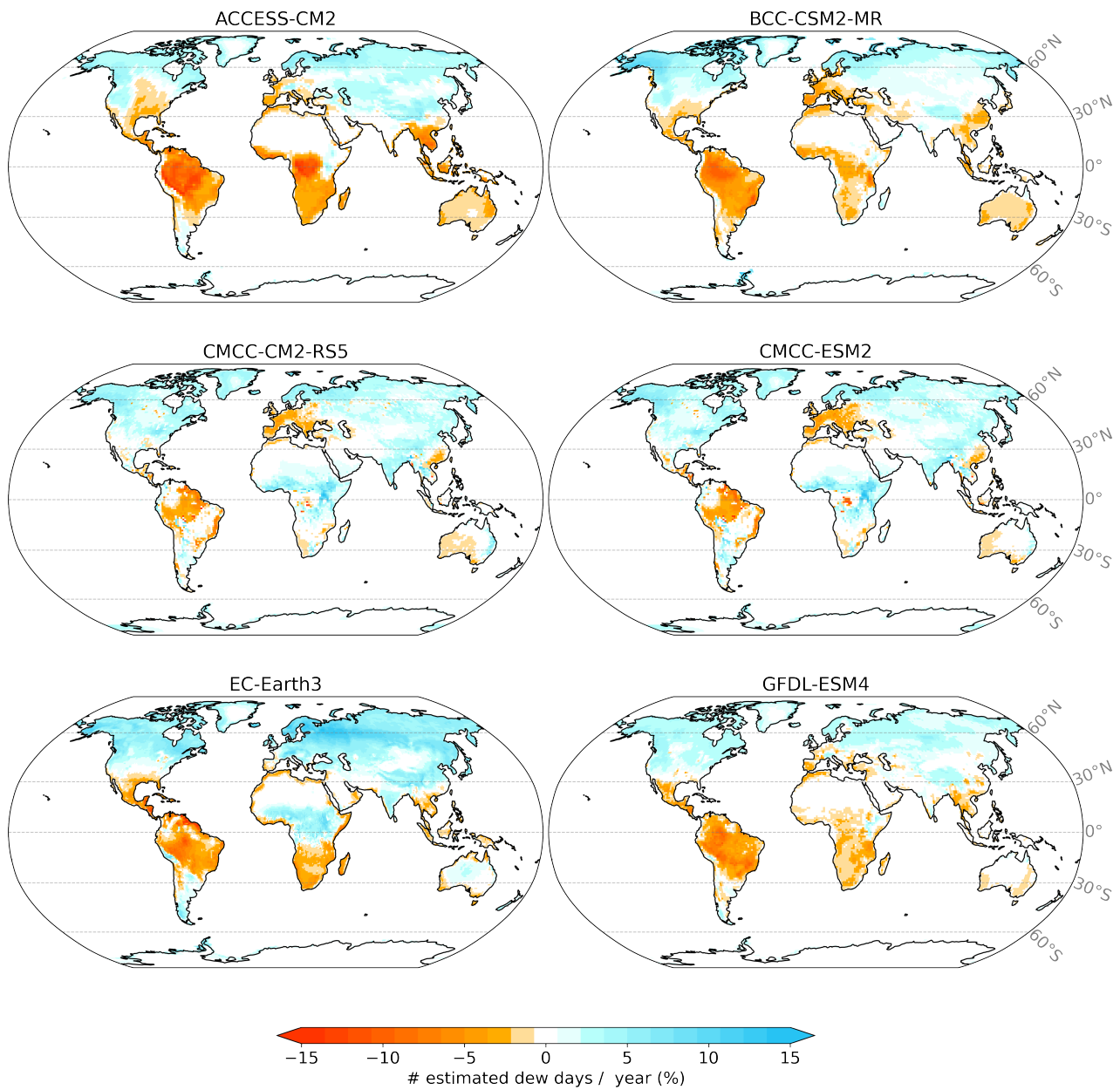


**Figure 11:** Change of the annual number of estimated dew days from 1950-1980 to 2070-2100. All models are shown alphabetically from the top left to the bottom right panel.

and CMCC-CM2-RS5 as well as CMCC-ESM2, show a cold bias in air surface temperature (*tas*) (Cherchi et al., 2019). The latter case could be more favorable for dew due to a faster reached dew point temperature. Therefore, the differences, e.g., in India, may partly be explained by a bias in either *tas* or precipitation.

Additionally, CMCC's models are negatively biased in temperature in areas starting north of the Congo Basin toward 30°N (Cherchi et al., 2019), i.e., there are reportedly warmer temperatures than simulated in the models. It is within the realm of possibility that the resulting increase in estimated dew days is less concise since, with colder temperatures, dew point temperature can be reached faster. Yet, considering air surface temperature by itself is not a very robust evaluation for dew formation.

According to Döscher et al. (2022), EC-Earth3 has a rather robust precipitation pattern but with some difficulties in parts of the tropics, like the majority of the other models (Bi et al., 2020; Wu et al., 2019; Cherchi et al., 2019). As already mentioned, precipitation influences the number of countable days. If the models overestimate the countable days (negative precipitation bias), there are more possibilities for dew to form and vice versa. A bias is detected in the historical period and may not apply to projections. So in these areas, changes must be viewed more cautiously.

In summary, models show differences regarding regional changes. However, matching patterns are distinguishable across the models with different atmosphere circulation model. Some models show more similarities than others. ACCESS-CM2, BCC-CSM2, and GFDL-ESM4 show more similarities than CMCC-CM2-RS5 and CMCC-ESM2, and EC-Earth3 shows the strongest divergence from all models.

### 3.2.3 Global patterns relative to counted days

Countable days can influence the results on estimated dew days in some areas, as mentioned in Section 3.2.2. Figure 12 illustrates that especially the Amazon, the tempered zone of Eurasia, and the Eastern USA are influenced to a certain extent, as shown by the change in estimated dew days relative to counted days from 1950-1980 to 2070-2100. The shown multi-model mean includes stippling in areas where all models agree on the change.

The three models ACCESS-CM2, CMCC-ESM2, and EC-Earth3 are chosen each to represent the above mentioned groups of models and their patterns. In addition, they represent different trends in the global mean; CMCC-ESM2 and EC-Earth3 show an increasing trend, whereas ACCESS-CM2 has a declining trend in estimated dew days (Fig. 9c).

In contrast to the estimated change in Fig. 11, the change relative to counted days in the estimated

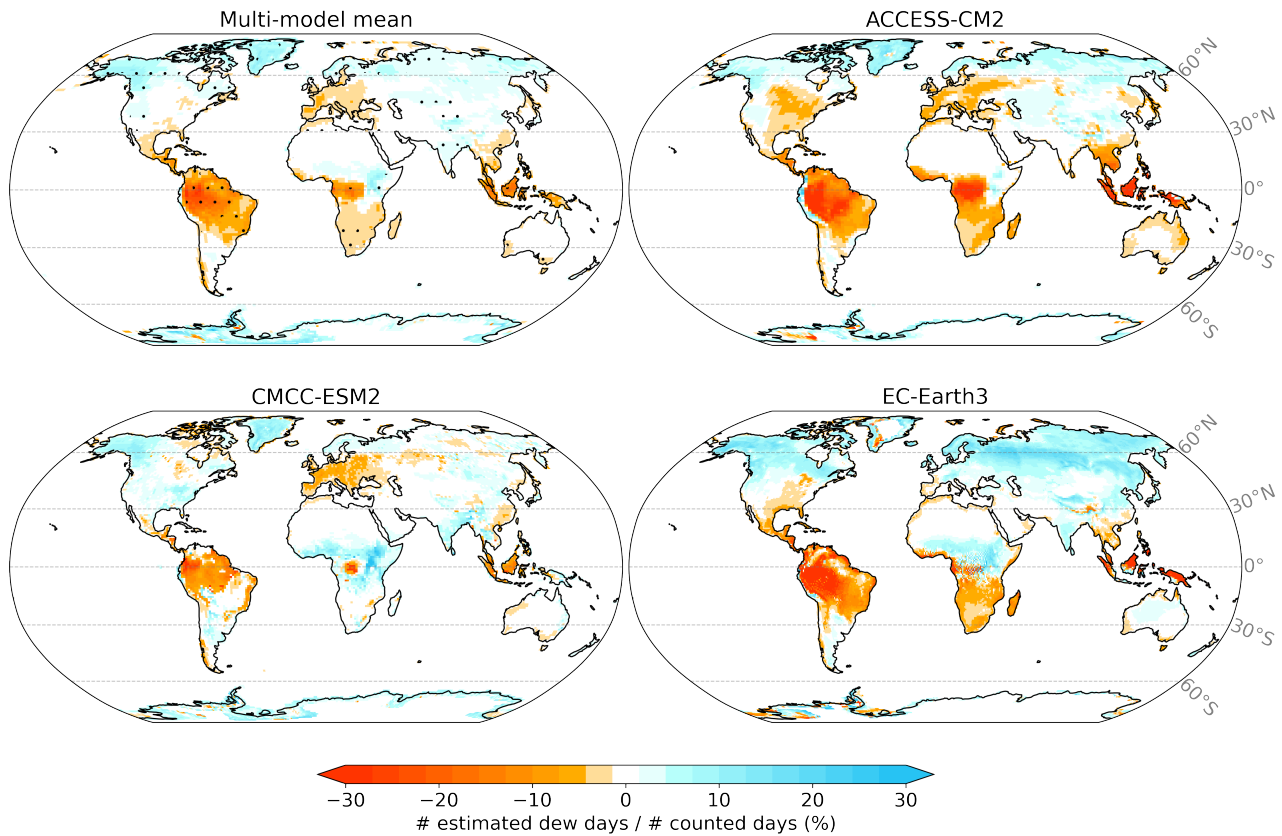


**Figure 12:** Change of the climate in the annual number of estimated dew days relative to counted days from 1950-1980 to 2070-2100. The top left panel depicts the multi-model mean, the top right panel shows the model ACCESS-CM2 (representative for BCC-CSM2-MR and GFDL-ESM4), the bottom left panel shows the CMCC-ESM2 (also representative for CMCC-CM2-RS), and the bottom right panel depicts EC-Earth3. The stippling in the panel with the multi-model mean indicates areas where all models agree on the trend.

dew formation is evolving towards a negative number in the Eurasian temperate zone and Eastern USA (Fig. 12). It is assumed that the temperature greatly impacts the estimated dew days above  $45^{\circ}\text{N}$ . Warming in such regions influences the contrasting responses of the models in estimated dew days above  $45^{\circ}\text{N}$  by two factors. First, there are more days on which dew can even form because the number of days with temperatures above  $0^{\circ}\text{C}$  increases. This results in an overall increase in the absolute number of dew days shown in Fig. 11, whereas there is a decrease in the number of dew days relative to the counted days (Fig. 12) in the model groups of ACCESS-CM2 and CMCC-ESM2. Second, the Clausius-Clapeyron equation shows that the water holding capacity increases with warmer temperatures. For temperatures in low ranges, saturation vapor pressure ( $e_s$ ) does not increase as fast as temperature, so that dew point temperature ( $T_d$ ) is reached faster than in already warm areas. This condition is more favorable for dew formation. However, the faster reached dew point temperature may appear mainly in Eastern Asia as well as North America, where an increase in relative humidity is predicted (Byrne and O’Gorman, 2013), and less in the noted area in tempered Eurasian of decreasing dew frequency. According to Byrne and O’Gorman (2013), the noted area shows a declining relative humidity which is less favorable for dew formation. In other words, the estimated increase in dew days

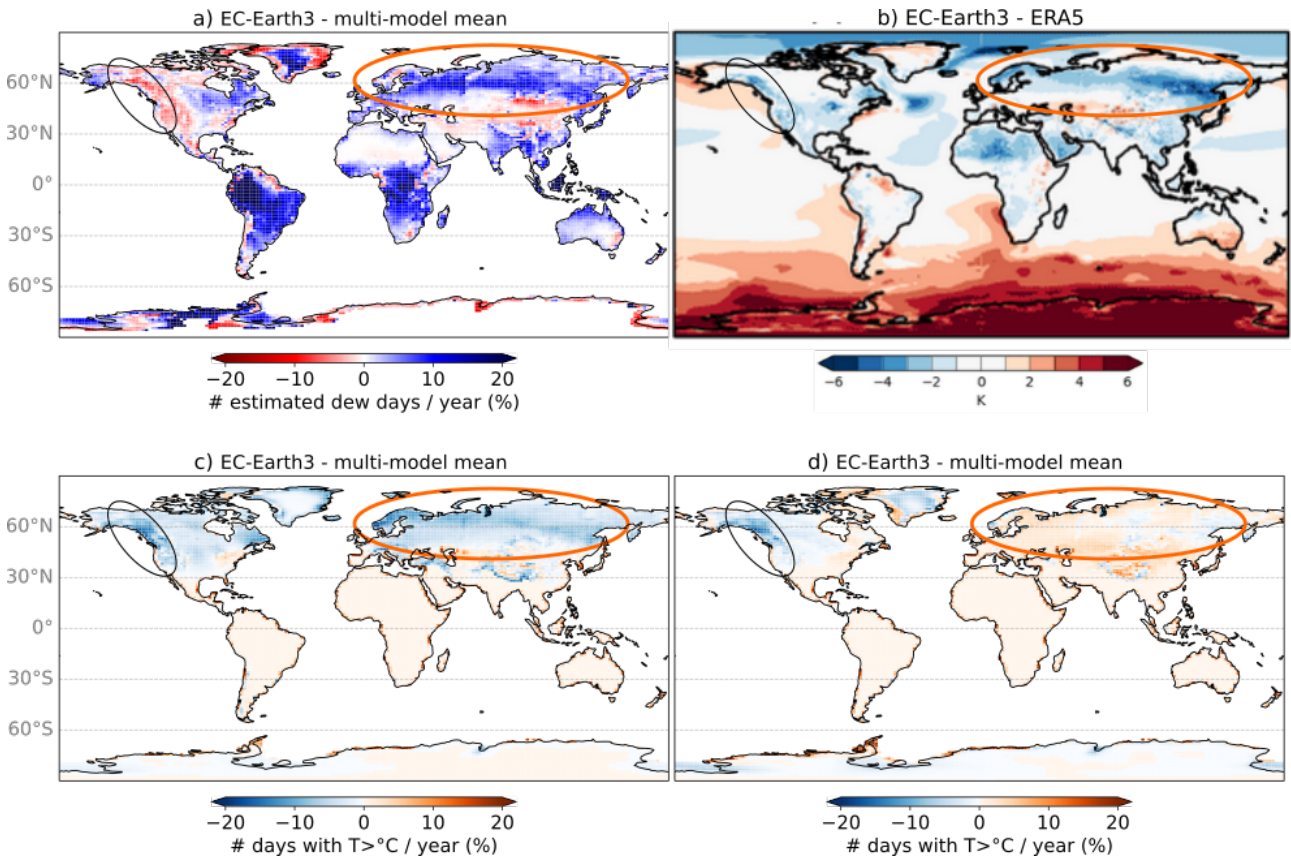


**Figure 13:** a) Bias of EC-Earth3 compared to the multi-model mean in the average of dew days relative to counted days and b) EC-Earth3 model bias compared to ERA5 ensembles in air surface temperature (Figure retrieved from Döscher et al. (2022); Fig. 5). Please note that a) is in days / year (%) and b) in Kelvin. c) shows the bias of EC-Earth3 to multi-model mean in mean of number of days with temperatures above 0°C of the period 1950-1980 and d) the period 2070-2100.

in Eurasia (Fig. 11) is partly due to the increasing number of counted days (Fig. 12). The number of estimated dew days even decreases partly in this area (Fig. 12), which is possibly caused by a lower atmospheric water vapor availability (Byrne and O’Gorman, 2013).

Contrarily, EC-Earth3 shows a strengthening in the number of estimated dew days across Eurasia, even though there are higher numbers of counted days in the second period (2070-2100) compared to the first period (1950-1980). The increase is possibly influenced by a negatively biased air surface temperature in the historical period (Döscher et al. (2022), Fig. 5b; Fig. 13). Figure 13a illustrates that the deviation in estimated dew days of EC-Earth3 from the multi-model mean overlaps with the model bias in *tas* in Eurasia (Fig. 13b orange circle). In the historical period (not shown), the deviation in estimated dew days of the model EC-Earth3 from the multi-model mean is negative. It turns positive in the projected period (Fig. 13a). The cold bias may only affect the historical period, since the deviation of EC-Earth3 from the multi-model mean in days of  $T > 0^\circ\text{C}$  is negative (Fig 13c), but  $T > 0^\circ\text{C}$  shows a positive deviation in the projected period (Fig 13d).

The change (from Fig 13c to d) indicates stronger warming in the noted area in EC-Earth3. The

initially colder temperature in EC-Earth3 may be no longer expected in the projection. This indicates a stronger temperature increase than projected by other models. In the case of EC-Earth3, the apparently stronger temperature increase compared to other models may be followed by a stronger increase in atmospheric water vapor. These conditions and the high diurnal temperature range in high latitudes are favorable for dew to form, and therefore, EC-Earth3 shows a stronger increase in dew days.

A somehow similar effect can be assumed on the West coast of North America (Fig.13 black circle). In this case, the cold bias may still be in the projected period (Fig.13d). This then could cause the lower number in estimated dew days of EC-Earth3 than the multi-model mean (Fig.13a). This coincides with the above stated assumption that dew days may increase stronger, due to a supposedly stronger increase in temperature.

It can be concluded that the stronger increase in the number of estimated dew days of EC-Earth3 in comparison to other models may be due to the stronger increase in temperature. EC-Earth3 is the only model showing such a strong increase in dew frequency. In combination with the reportedly cold bias, one can assume that in EC-Earth3, the change might be overestimated.

Unlike the increasing trend in Eurasia, there is a robust decrease in estimated dew days in the Amazon which gets even more pronounced when only the counted days are considered. The decrease in countable days originates from increased days without precipitation (Fig. 14).

In the Southern Hemisphere, including latitudes up to 30°N, the number of counted days is mainly determined by the number of days without precipitation, whereas in areas above 30°N, days with temperatures above 0°C have an additional influence. Notably, the models mostly agree on the growth of countable days in the northern part which is mostly based on temperature increase and decreasing days without precipitation; however, they strongly diverge in the southern part.

The temperature change mainly affects the counted days in the North, since in the South, there are only few regions that show temperatures below 0°C in today's climate; therefore, there is only a minor change in counted days influenced by temperature.

In summary, the global mean illustrates that dew days increase over time. However, this is mainly due to the rise in the number of counted days. Even though dew days relative to the number of counted days do not increase everywhere over time, there are clear tendencies to either decrease or increase on a regional scale. The models disagree in large parts of the world. However, it can be said that the declining prediction in estimated dew days is robust in the tropics (such as the Amazon, Congo Basin, and parts of South East Asia). The increase in the northern subpolar and polar regions is also

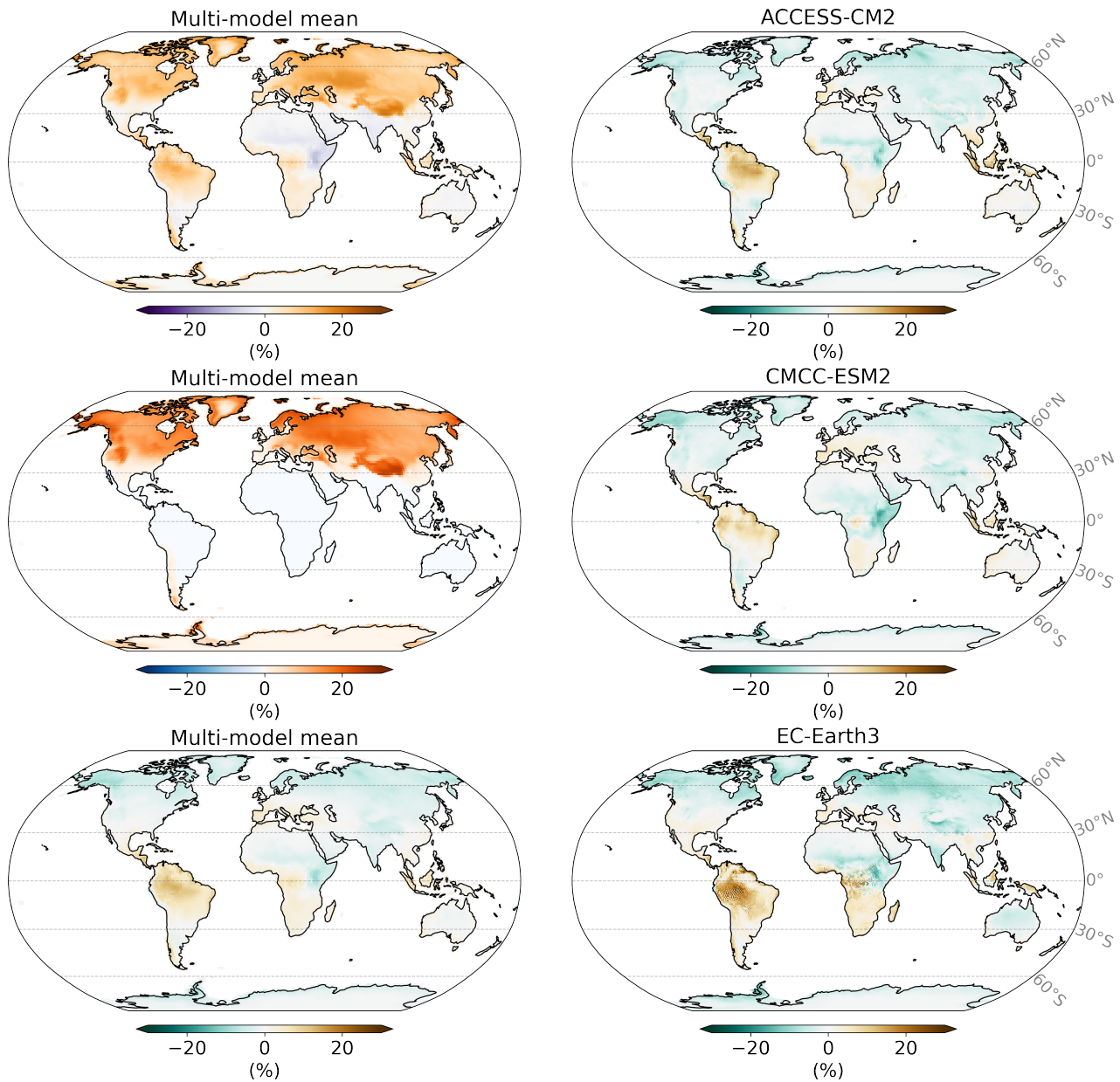


**Figure 14:** Change in the number of counted days, days with temperature above 0°C, and days without precipitation on the left are shown as multi-model mean. On the right, the change in days without precipitation is shown for the models ACCESS-CM2, CMCC-ESM2, and EC-Earth3 from top to bottom.



a robust feature in the six chosen models. The reasons for the changing trends differ for each region. The changes in the subpolar regions originate mainly from a higher amount of counted days. The tropical regions, e.g., the Amazon, actually show a decrease in estimated dew days in terms of both absolute and relative frequency.

### 3.3 Zonal and regional trends in estimated dew days

Section 3.2.2 showed that some climate zones are distinguishable within the changing patterns. For instance, in the areas around the equator, a rather robust negative trend is predicted across all models. These zones are also indicative of biomes; using the example above, these are mainly regions covered in tropical forests. First, we look at the zonal mean, and then we analyze the sensitivity of the different biomes in more detail. The analysis compares the mean of a historical period (p1: 1950-1980) to a projected period (p2: 2070-2100).

#### 3.3.1 Changes in the zonal mean

The zonal mean is relatively robust across the models, with slightly more differences among the models in the Southern Hemisphere compared to the Northern Hemisphere, shown in Fig. 15. The figure shows the multi-model mean, whereas the different models represent slightly transparent lines.

A distinguishable pattern can be identified in the zonal mean, which is based on the average climate in terms of temperature and water vapor. The number of estimated dew days peaks at the equator in both periods; in p1, on average, 67 days or 19% and p2 60 days or 15% (Fig 15a+b). It peaks not only in the multi-model mean but also across all models. This is due to warm temperatures and high evapotranspiration. The resulting high relative humidity at the equator leads to a favorable condition for dew to form.

The local minima in estimated dew days are around the subtropics (20°N, 25°S). There, the (tropical) jets and trade winds cause an influx of dry air, causing a higher water vapor pressure deficit ( $VPD = e_s - e$ ) and, hence, low relative humidity (Byrne and O’Gorman, 2013). In other words, even though the diurnal temperature cycle in the subtropics has a high amplitude which is favorable for dew, the relative humidity seems to be too low for dew to form. In this area, both periods show similar values; therefore, there is no projected change for the future. The estimated dew days increase again in the temperate zone. It reaches local maxima in the subpolar regions (60°N and 50°S), where the diurnal temperature cycle has a high amplitude (favorable to reach dew point temperature), and the relative humidity is higher than in the subtropics (Byrne and O’Gorman, 2013).

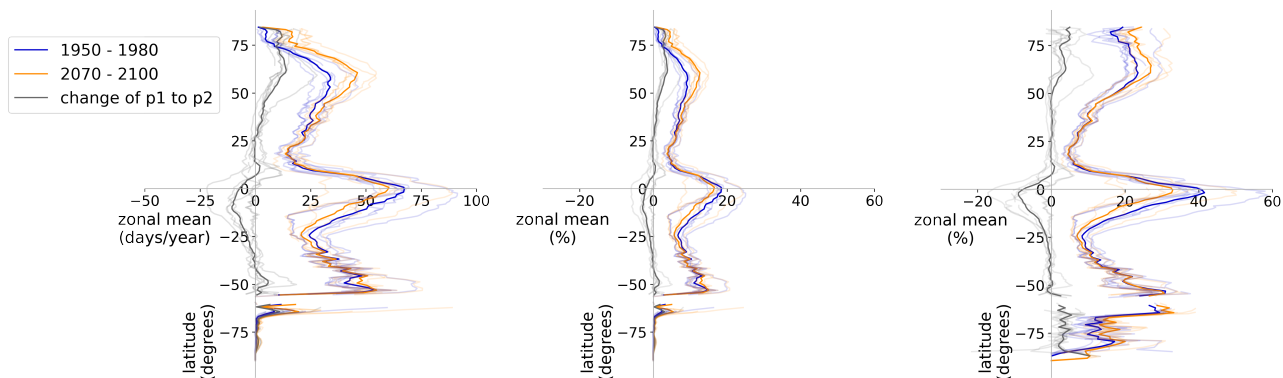


**Figure 15:** The multi-model zonal mean of the mean over period 1 (1950-1980) in blue, period 2 (2070-2100) in orange, and the difference of period 1 to period 2 in gray. The variability of the models is shown in a more transparent color. a) Depicts absolute estimated dew days, b) estimated dew days relative to days in a year, and c) relative to the number of counted days shown.

Even though the amount of dew days peaks at the equator, the number of estimated dew days mostly increases (gray) with time in the northern (sub)polar region (+14 days or +4% in multi-model mean, and +2 to +6% change in the models). The highest decrease in the zonal mean between the two periods p1 and p2 is at 10°S. The decline is, on average, about 10 days or 2% (multi-model mean), varying from 1% to 6% depending on the model. Besides this, the negative trend slowly turns into a positive trend with increasing latitudes around 25°N and 35°S. After a peak, it slowly decreases until zero change when the polar land area ends.

The resulting increase in the northern (sub)polar zone is already distinguishable in the rise in the global pattern (Section 3.2.2; Fig. 11) and the decline at the equator. However, the multi-model mean increase of around 50°S is not clearly noticeable in the global plots; there is only a small patch of land at the southern end of South America, which does not stand out on a global pattern.

Eventually, considering the zonal mean relative to counted days illustrates that countable days change to a certain degree, especially in the polar and subpolar regions and at the equator (Fig. 15c). Where areas between 10 - 25°N and 20 - 30°S do not show a major difference in contrast to Fig. 15b, the above mentioned areas highly enlarge in percentage in both periods. In both periods, the (sub)polar zone shows an increase in estimated dew days of +14% in the Northern Hemisphere and +17% in the Southern Hemisphere. At the equator, the percentage changes from 19 to 41% in p1 and 15 to 33% in p2 (+22% and +18%, respectively).

Although the zonal mean in estimated dew days depends on counted days, the increase from p1 to p2 is steady in (sub)polar regions, and a decreasing trend at the equator is enlarged by around 4%. Here, the change is due to an increasing number of counted days, particularly those without precipitation. Thus, some areas around the equator face not only less precipitation but also fewer estimated dew



days.

A decreasing number of estimated dew days can be caused by a drier atmosphere. For instance, the negative trend in estimated dew days between 5°N to 25°S overlaps with the predicted decrease in relative humidity (Byrne and O’Gorman, 2013, 2016; O’Gorman and Muller, 2010). Among other latitudinal zones, Byrne and O’Gorman (2016) conclude a decrease of about -0.5% to -1% °C<sup>-1</sup> over land from 1976-2005 to 2070-2099. Moreover, Simmons et al. (2010) already show a decline in relative humidity in the equatorial regions between 1989-1998 and 2004-2008.

There is a disagreement at latitudes above 60°N, where O’Gorman and Muller (2010) do not report a decrease in relative humidity over land, which would support the increasing trend in estimated dew days. On the other hand, Byrne and O’Gorman (2016) project a decrease in relative humidity by -0.3% for each 1°C warming compared to the historical period in zonal mean.

The disagreement indicates the difficulties in explaining the change in estimated dew days when simply considering atmospheric water vapor. Thus, an additional driver, such as temperature, must be considered in the polar region. Indeed, not only atmospheric dryness is important to analyze but also the diurnal temperature cycle and the associated surface cooling. The daily temperature range is driven by many factors, such as cloud cover, greenhouse gases (including water vapor), or evapotranspiration. In high latitudes, a lower temperature range in winter is expected. This might be associated with a higher cloud cover, but in summer, the diurnal temperature cycle will be more pronounced in the future (Lindvall and Svensson, 2015). According to Lindvall and Svensson (2015), the minimum temperature is influenced by a lower cloud cover which is favorable for surface cooling at night. Since these regions mostly have temperatures below 0°C in winter, the days may only account for a small number of dew days (given by the herein set restrictions). The lower temperature range in winter has only a minor effect on the change in the estimated number of dew days. Nevertheless, the higher temperature range in summer could positively influence the estimated dew days. In other words, increasing summer temperature ranges associated with a low fraction of cloud cover may be more influential on dew formation than decreasing temperature ranges in winter.

Indeed, surface cooling and, therefore, the interaction between the diurnal temperature range and cloud cover is one of the main drivers for dew formation. Vuollekoski et al. (2015) concluded that dew formation is mainly inhibited by too little surface cooling due to cloudy or foggy conditions. It is important to note that the aforementioned study relates to dew formation on artificial surfaces, and, therefore, it may differ slightly from natural surfaces. However, similar to dew formation on artificial surfaces Ritter et al. (2019) agree on the latter in natural environments. Fog and cloud cover are associated with atmospheric water vapor. The nonclear sky inhibits longwave radiation from escaping and

can cause a warming atmosphere. As a result, the higher atmospheric water vapor may inhibit surface cooling. In view of this, the potentially slower increase in specific humidity compared to temperature may influence the cloud cover. Lower cloud fraction affects the surface cooling less negatively. This then may be beneficial for dew formation at high latitudes in regions above 60°N.

In summary, the most pronounced changes are in the tropics and the northern polar regions. The tropics show a decrease in estimated dew days from 1950-1980 to 2070-2100. The decrease is expected to be caused by a drying of the atmosphere. The northern high latitudes show an increase in estimated dew days with time. The supposed decrease in relative humidity (Byrne and O’Gorman, 2016) may be beneficial for radiative cooling and can thereby enhance dew formation (Ritter et al., 2019; Vuollekoski et al., 2015).

### 3.3.2 Impact of different biomes on dew frequency

The zonal mean is indicative of different climate characteristics based on the latitudinal location. However, climate and, thus, vegetation strongly depend on local features, and anthropogenic climate change makes some areas more sensitive to dew formation than others. In order to understand these effects better, this section focuses on biomes grouped by distinguishable ecosystems. The locations of the different biomes are defined according to satellite data (Section 2.1.2).

In general, an increase of estimated dew days occurs in biomes predominant in the Northern Hemisphere above 24°N (Fig. 16). Between 50%-75% of grass and crops and at least 75% of tundra and extratropical forest areas are affected. Areas in the tundra show the highest increase across most models (except EC-Earth3). The boxplots for each model in Fig. 17 show the distribution of the change in estimated dew days from p1 (1950-1980) to p2 (2070-2100) for the different biomes.

The increasing trend of dew days in the temperate North is partly due to the rising temperature and the number of counted days, as already discussed in Section 3.2.3. Note that this mainly applies to areas in extratropical forests. This leads to the hypothesis that there might be a kind of vegetation feedback on dew formation.

In general, the VPD increases with higher temperatures which induces a higher evapotranspiration rate (Dai et al., 2018). In biomes such as the tundra, the potential evapotranspiration increases (Scheff and Frierson, 2015) and, thus, might shrink the VPD in the atmosphere because, on average, enough water will be available to keep up with it eventually. There is an ongoing exchange of water between the atmosphere and soil. The evaporating soil moisture keeps the relative humidity high enough for favorable dew conditions, even though the temperatures increase faster than the specific humidity (as

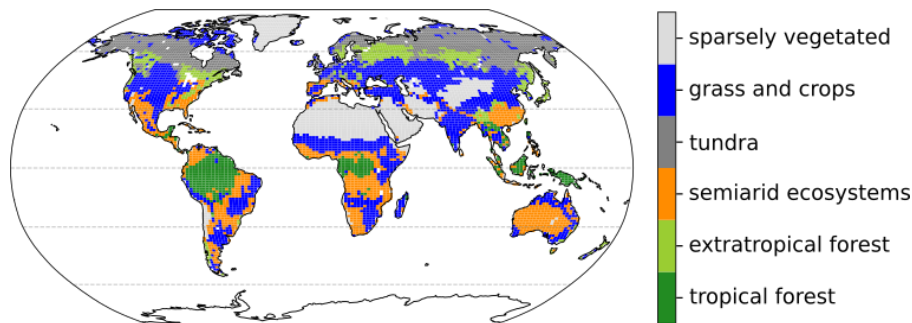


**Figure 16:** The map of biomes based on MODIS satellite data (Section 2.1.2).

discussed in Section 3.3.1).

Although the evapotranspiration rate depends on the vegetation cover, the prominent vegetation covers in the North (e.g., grassland and summer green forest) show similar evapotranspiration rates among themselves except for coniferous forests (a subgroup of extratropical forests) (Zha et al., 2010). They show lower evapotranspiration rates, especially in water-limited regions (Zha et al., 2010). However, the northern areas are predicted to get wetter in the future (Cook et al., 2020; Scheff and Frierson, 2015) with increasing water runoff, but a projected decrease in soil moisture (Cook et al., 2020). Evapotranspiration may contribute to the increase in estimated dew frequency in areas above  $24^{\circ}\text{N}$ , but the difference in the extent of increase among vegetation types in this area is not explained.

Further, the diurnal temperature range may influence the estimated number of dew days (as already discussed in Section 3.3.1 with a focus on high latitudes). Lindvall and Svensson (2015) suspect a smaller amplitude over coniferous forests in the Northern Hemisphere in future winters. They further state a contrary projection for coniferous forests in future summers, i.e., a favorable condition for dew days due to larger diurnal temperature cycles. This might affect all extratropical forests in the Northern Hemisphere since they usually consist of mixed forests. As already discussed in Section 3.3.1, we assume that the summer months have a stronger influence on the dew days frequency than the winter months. In winter, the lower amplitude correlates with an increase in the minimum temperature. The increase is influenced by downwelling longwave (Lindvall and Svensson, 2015). The rise of minimum temperature causes an increase in counted days. The results show an increase in dew days, but extratropical forests seem more sensitive to the change in counted days than other biomes. The projected smaller temperature amplitude over coniferous forests than other biomes may partly explain the higher sensitivity of dew days in northern forests in the future, particularly in Eurasia. However, it is difficult to assess the driver explicitly. The changes are influenced by many different drivers and their feedback mechanisms, which need to be analyzed separately.

Concretely, it can be said that there is a clear increase in dew days in the tundra, the extratropical

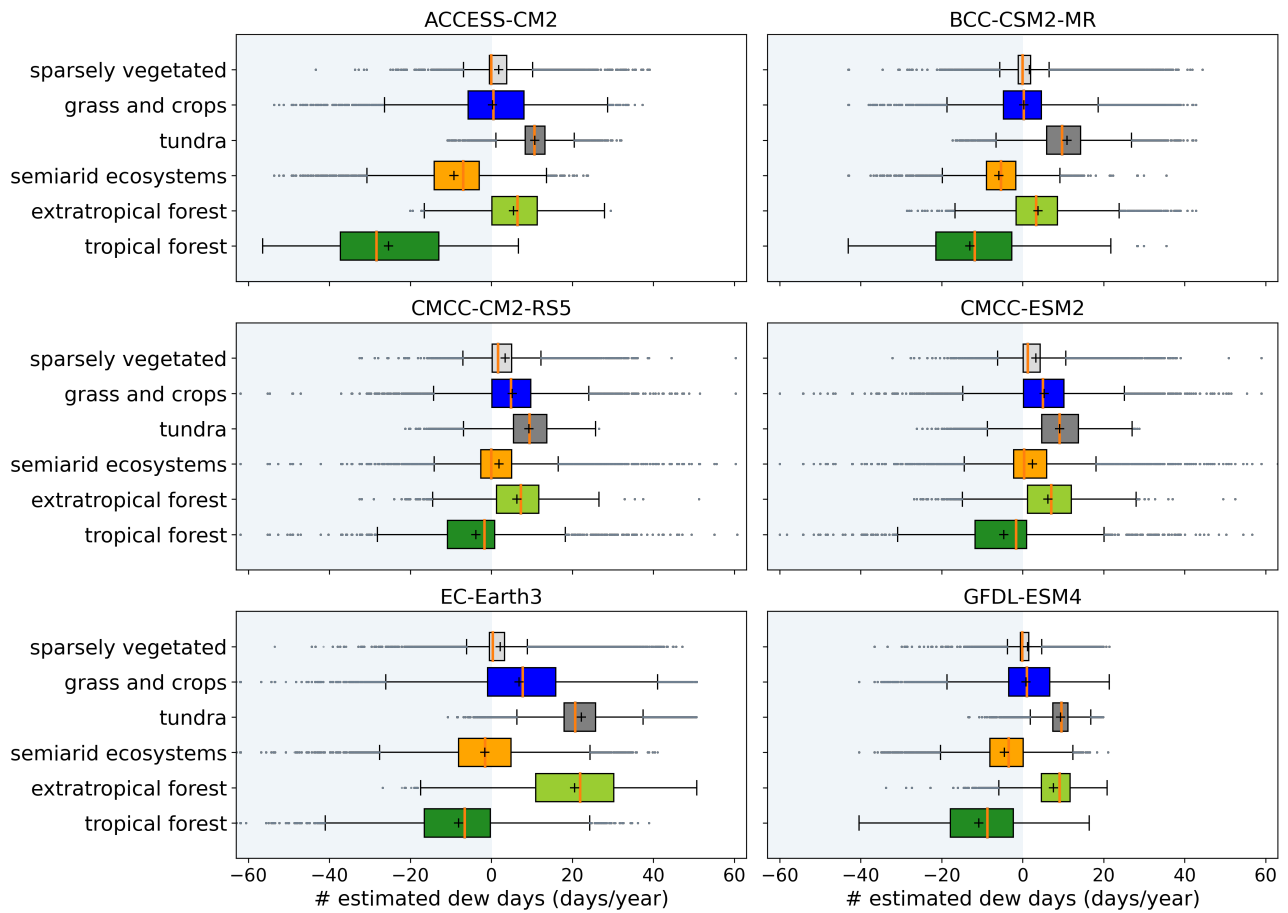


**Figure 17:** The absolute change of the climatic mean in dew days for each grid cell according to the biome from 1950-1980 to 2070-2100. All models are alphabetically listed. The data excludes the Antarctica.

forests, and in grass and crops in the Northern Hemisphere. In extratropical forests, the increase in minimum temperature in winter increases the number of counted days, and thus, affects the estimated number of dew days.

The biomes are sensitive to changing conditions. An ecosystem can either be positively or negatively affected. For instance, higher dew occurrence can result in lower crop yields since, in humid areas, the probability of pests and plant diseases increases (Nath, 2021). On the other hand, dew can be of value in rather water-stressed areas as an additional water source (Yokoyama et al., 2021), whereby these areas can be relieved to a certain extent (Berry et al., 2019; Kidron and Starinsky, 2019).

Ahlström et al. (2015) defines arid regions, urban build-ups, and ice-covered regions as sparsely vegetated areas. Interestingly, summarized as biome, they show similar trends to the previously discussed biomes. In 50%- 75% of these areas, the number of dew days increases (Fig 17). The considered CMCC models show a decrease in estimated dew days only in 25% of the area. The other models show a decrease in dew days in 50% of the areas, where half of this 50% shows almost no decrease. Antarctica is a distinguished ecosystem, therefore, not included in sparsely vegetated areas in this

analysis. Antarctica would bias the results leading to a distribution close to zero with many outliers.

It is noticeable that mainly sparsely vegetated biomes with cold winters show a strong increase in dew days, e.g., Northeast China, the coast of Greenland, and areas East of the Caspian Sea (Fig. 18a). Although the minimum temperatures increase in winter and, therefore, the number of counted days, it seems not to influence the dew day occurrence (not shown). Hence, it can be assumed that changes are not caused by increased days above 0°C.

Hao et al. (2012) concludes an increase of dew days in a specific region of the Taklimakan Desert in Northeast China for summer and early fall (June-October). The opposite is shown by Dou et al. (2021) by measuring at multiple places in the Taklimakan Desert for the entire season; the authors predict a decrease in dew days due to near surface air warming and associated decrease in relative humidity. The disagreement of both in situ studies could result from the different locations and periods. The models project similar to Hao et al. (2012) an increase in estimated dew days. Our results in this area might need to be looked at more critically.

Projections of precipitation days from p1 to p2 show an increase north of 30°N (Fig 14). The projections also show an increase in temperature, causing favorable conditions for dew days. In low precipitation areas, the atmospheric water vapor is additionally driven by evapotranspiration, but the evapotranspiration rate shrinks with decreasing vegetation cover (Wang et al., 2018). The water availability decreases and dew formation might be more sensitive to changing conditions. For instance, in North Africa, the trends are deviating. A decrease in the northern Sahara is expected and an increasing trend in the southern Sahara (Fig. 18a). Yet, the increase in the southern part is not robust regarding the six models (Section 3.2.2 and Fig. 11). There is a robust decrease at the northern border of the Sahara.

A similar trend is expected by Feng and Fu (2013), they state a global expansion of dry land and, in the case of North Africa, northern migration of drylands; i.e., the southern border of the Sahara is expected to become wetter and the northern border dryer. The analysis by Feng and Fu (2013) is partly based on atmospheric CMIP5 data. Since the analysis of estimated dew days is based on atmospheric conditions, namely, air surface temperature and dew point temperature, the results of both studies can be expected to be similar. Furthermore, a range of models based on land water storage within CMIP5 and a RCP8.5 scenario also support the assumption of drying at the northern border of the Sahara (Jensen et al., 2019). In other words, the mentioned studies support the assumption of a decrease in the estimated number of dew days in North Africa. The increase in the southern Sahara is less robust. Jensen et al. (2019) shows a less clear wetting trend. It emphasizes that models have difficulties predicting water-related changes in this region; therefore, the increase in dew days may not

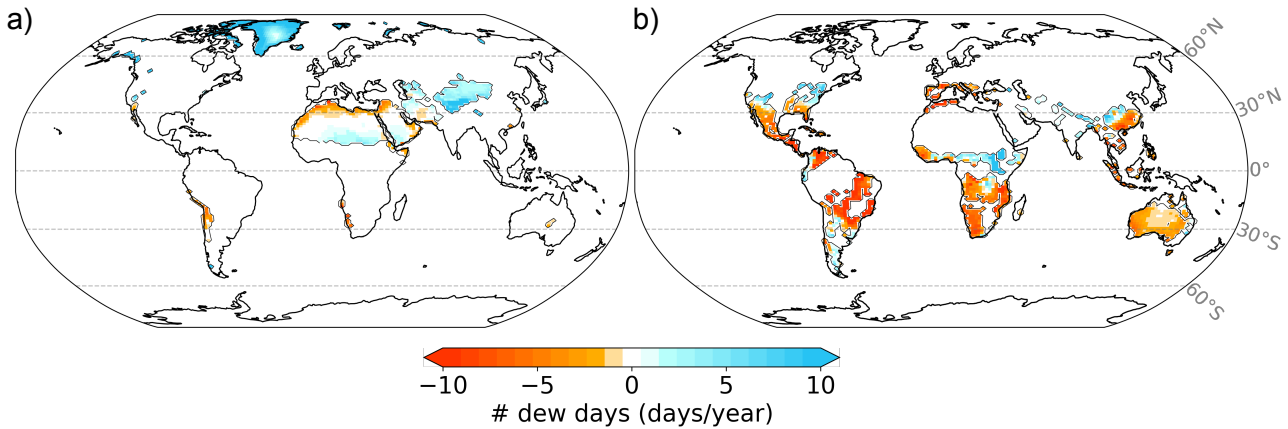


**Figure 18:** The change of the multi-model mean in the number of estimated dew days from 1950-1980 to 2070-2100 with a focus on the biome a) *sparsely vegetated* and b) *semi-arid ecosystems*.

be robust.

Even though evapotranspiration shrinks with decreasing vegetation cover (Wang et al., 2018), it may still be an important driver for dew formation in dry areas. With increasing temperatures, the water holding capacity of air increases, which can enhance evapotranspiration. In humid areas, evapotranspiration can increase; however, the changes may negatively affect dry regions. Not only North Africa shows a dividing trend in the estimated number of dew days, but also biomes of semi-arid ecosystems where a decrease of about 50% up to 75% of the affected areas is expected. The above discussed trend in North Africa also affects the results in semi-arid ecosystems (Fig. 18b). Additionally, there is a larger variation among models due to a disagreement in North America.

Further, Feng and Fu (2013) and Jensen et al. (2019) project a drying in North America. This would support the assumption that a decrease in relative humidity causes a decrease in dew days. The decline in dew days may be more pronounced in this area than shown here. Berg and McColl (2021) show the resilience of ecosystems under water stress by including ecohydrological effects, such as stomata responses and soil moisture, all of which are also factors of dew formation. With an increased water use efficiency of plants, less transpiration takes place, and thus, the atmospheric dryness could increase (Berg et al., 2016). This would then enhance the shown decrease of dew formation in North America. On the other hand, soil moisture can also create dew (dew rise) which may increase the number of dew days, but this is not explicitly considered in this thesis.

The differences between the biomes' semi-arid ecosystems and sparse vegetation may show the resilience of vegetation to drying conditions. Semi-arid areas have a higher vegetation cover and may decrease in evapotranspiration rates with drying conditions. A dryer atmosphere may lead to a decrease in dew occurrence. Sparse vegetation biomes have a low vegetation cover. The evapotranspiration fraction is less controlled by vegetation; Therefore, it may lead to an increase in the number of estimated dew

days. However, the resilience of an ecosystem is still a topic of debate (Feng and Fu, 2013; Berg and McColl, 2021).

In tropical forests, the models agree on a decreasing trend of estimated dew days which will be discussed in more detail in the next Section 3.3.3 with a focus on the Amazon. In summary, the biomes prominent in northern mid and high latitudes show an increase in estimated dew days. This seems to be caused by higher water availability in these regions. Extratropical forests have higher sensitivities to counted days which might be related to a lower amplitude in the diurnal temperature in winter. Evapotranspiration affects wet areas less than dry areas. Evapotranspiration may cause a change in semiarid ecosystems and dry, sparsely vegetated biomes. The latter may show higher evapotranspiration rates due to lower ecohydrological response to warming conditions.

### 3.3.3 Seasonality in the Amazon

The previously shown results indicate a strong response to changing conditions in tropical forests. For many reasons, the Amazon is interesting to analyze because it has a major impact on the global climate and its change. Since the results in the Amazon are consistent among the models (discussed in Section 3.2; Fig. 11 and 12), this region will be analysed in more detail. In the following section, only the multi-model mean will be discussed.

A season in the Amazon spans six months and can be separated into a wet (December-May) and a dry (June-November) season. The two seasons are defined based on precipitation rates (Binks et al., 2019). In the historical period, about 18% of the days in the wet season and 16% of the days in the dry season were favorable for dew to form in the Amazon, as shown in Fig. 19. In Figure 19, seasons are indicated in green for the wet season and brown for the dry season. It seems that in the wet season, there must be a high dew occurrence due to high water availability. Nevertheless, with more precipitation days, there are fewer possibilities for dew to form than in the dry season. By only considering estimated dew days relative to non-rainy days, dew is expected to form on 35% and 26% of the days in the wet and dry seasons, respectively (Fig. 19 *ii*). In other words, calculating estimated dew days relative to counted days negates the effect of increasing dew opportunities on the number of dew days. It eventually shows that dew is more prominent during the wet season than expected at first.

Even though the number of days without precipitation will rise in the future (Fig. 19 black dots) and, thus, the possibilities for dew to form will increase, the number of estimated dew days shrinks. In the decade 2090-2100, dew is expected on around 15% (wet season) and 10% (dry season) of the days. The

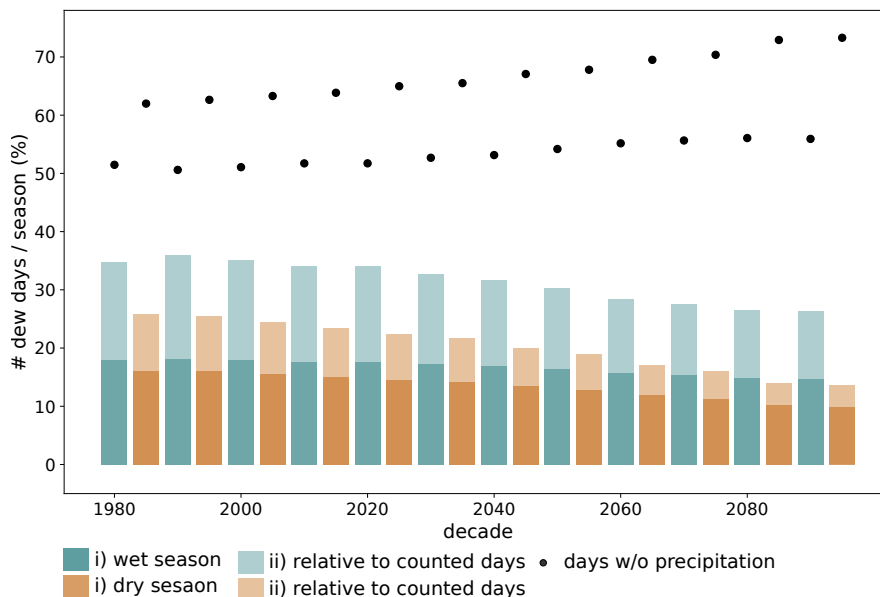


**Figure 19:** The decadal mean of estimated dew days in a season in the years 1981 to 2100. The wet season is shown in green and the dry season in brown. Lighter colors illustrate the days relative to counted days and the black dots the number of days without precipitation.

favorable days relative to counted days decrease even more. Especially in the dry season, the number of dew days drops by 12% from 26% to 14%, whereas in the wet season, dew days still account for 16% of the days (drops by 9%). Hence, the expected dew days drop stronger in the dry season when water stress is more probable.

Considering the above results, it may appear that estimated dew days are underestimated. According to an in situ study in the Eastern Amazon, dew forms on 36% of the days without precipitation (Binks et al., 2021). In the Amazon, the precipitation pattern is slightly negatively biased in the models (Bi et al., 2020; Wu et al., 2019; Cherchi et al., 2019; Döscher et al., 2022). The decrease in precipitation days might be overestimated, and therefore, it negatively influences the counted days. This could then account for some of the differences. On the other hand, a negative bias in the historical period does not necessarily mean that the projection shows the same bias. If the bias in the projection adjusts, the magnitude of the increase in days without precipitation may shrink. Since precipitation affects not only the number of counted days but also atmospheric water content, it could lead to an underestimation in the change of dew frequency.

Besides the effect of precipitation, models are negatively biased in evapotranspiration in the dry season (Baker and Spracklen, 2022; Baker et al., 2021) (Fig. 20b). Evapotranspiration is an important water source in the Amazon. Less evapotranspiration can lead to a dryer atmosphere and it can be less favorable for dew formation. This bias implies an underestimation of dew days in the dry season; thus, the decrease in dew days is maybe not as pronounced as shown here.



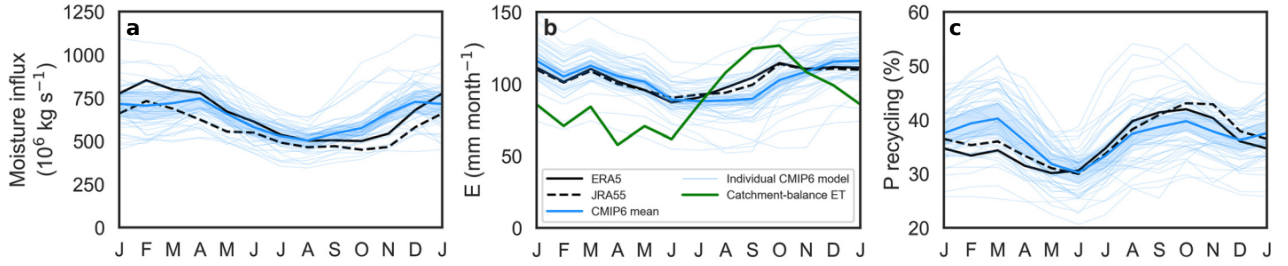


**Figure 20:** The expected moisture influx (a), evaporation (b), and precipitation recycling rate (c) according to Baker and Spracklen (2022). Figure retrieved from Baker and Spracklen (2022): Fig. 3.

Since dew highly depends on atmospheric water content, it is crucial to understand the water cycle in the Amazon. In the Amazon, the water balance is controlled by incoming moisture in the wet season (Fig. 20a), including a cascading cycle of precipitation and evapotranspiration (Staal et al., 2018; Marengo and Abril, 2006; Zemp et al., 2014). During the dry season, the moisture influx is at its minimum, and a high fraction of the precipitating water is recycled by a high evapotranspiration rate (Fig. 20b and c). The rate of precipitation recycling increases not only in the dry season but also further inland (Staal et al., 2018). The Amazon shows a complex water cycle that feeds itself. It results in a higher resilience against dry spells (Staal et al., 2018).

Dew days are influenced by precipitation recycling and evapotranspiration. Low evapotranspiration rates indicate less water availability in the atmosphere, which can negatively influence dew occurrence. Not only the water availability plays an important role, but also the diurnal temperature cycle. During the wet season, there is a higher fraction of cloud cover, which can reduce the nightly surface cooling and, therefore, may influence dew frequency negatively.

The decline in estimated dew days already starts in the 1980s and grows with time in both seasons, as shown in Fig. 21a. The Figure shows the decadal anomaly to each season's historical period (1950-1980). Again, the seasons are indicated in green (wet season) and brown (dry season). Each season is split into the first half (December, January, February (DJF) and June, July, August (JJA)) and the second half (March, April, May (MAM) and September, October, November (SON)) of the wet and dry season, respectively.

From the 2010s on, the decrease in the wet season is smaller than in the dry season (Fig. 21a *i*). This also applies for the number of estimated days relative to counted days (Fig. 21a *ii*). Including the seasonal anomaly in the number of counted days (Fig. 21b), one can conclude that a certain fraction of the decrease in estimated dew days is caused by the increase in days without precipitation. In this case, the number of days without precipitation (indicated by the black dots) is equivalent to counted days. Less precipitation might implicate less water availability in the atmosphere and, thus, less favorable conditions for dew to form.

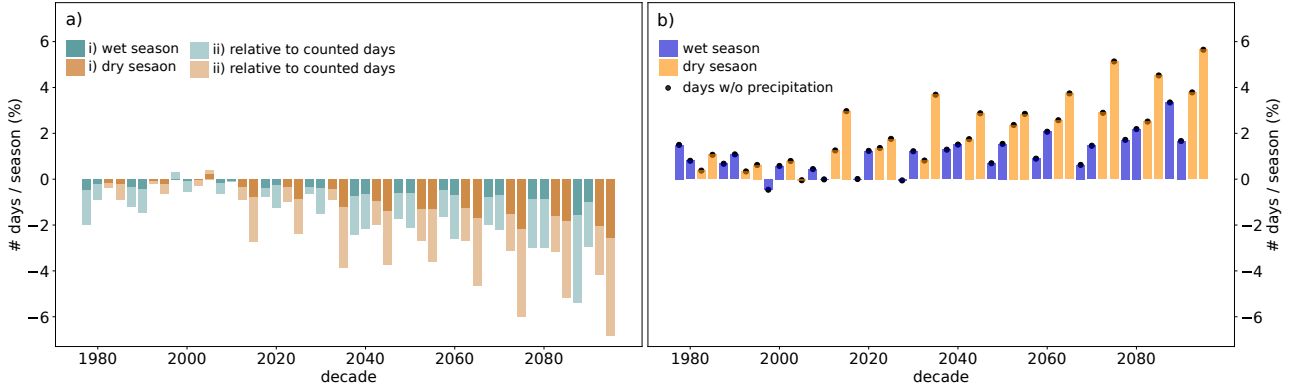


**Figure 21:** The decadal anomaly from 1981-2100 to the historical period (1950-1980) in a season. The wet season is shown in green and the dry season in brown. In panel a colors i) show the anomaly of the sum of dew days in a season and b) shows the anomaly of the sum of the counted days; the contribution of days without precipitation to the anomaly in counted days is shown by the black dots. In the panel a) the lighter colors (ii) illustrate the anomaly relative to counted days. The two seasons are additionally split into first half of the season (DJF and JJA) and second half of the season (MAM and SON).

Both seasons are expected to face drier conditions due to increased temperatures (Cook et al., 2020; Scheff and Frierson, 2015) and, thus, fewer dew days. By considering four seasons (DJF + MAM wet season and JJA + SON dry season) instead of two seasons, the dry season shows a more negative trend in the second half (SON) than the first half (JJA). Based on the evapotranspiration rate, possibly higher water stress is expected by the end of the dry season already today (Hasler and Avissar, 2007). Decreasing evapotranspiration rates indicate a drop in soil moisture and, therefore, lower water availability for the vegetation (Hasler and Avissar, 2007). In dry seasons, the water vapor-pressure deficit increases in the atmosphere due to the lower evapotranspiration rates. The higher VPD can lift evapotranspiration rates (Dai et al., 2018; Zhou et al., 2019). Yet, with the future change to lower evapotranspiration (Douville et al., 2021), might be due to increasing soil drought (Cook et al., 2020; Zhou et al., 2019), the water content in the atmosphere will shrink, and with it, the probability of reaching dew point temperatures. The result will possibly be a lower amount of estimated dew days.

Plants can overcome water-stressed periods by foliar water uptake (Berry et al., 2019). In the Amazon, dew contributes a high fraction to foliar water uptake in the early morning (Binks et al., 2019). With less dew occurrence, the water stress is more severe. Low soil moisture and the accompanying VPD can inhibit stomatal activity. This can enhance the drying of the atmosphere (Berg et al., 2016) and, thus, is even less favorable for dew to form. In other words, during the dry season, not only precipitation decreases, but also the estimated dew, which accounts for a high fraction of the canopy wetness (Binks et al., 2021) and, thus, foliar water uptake of the vegetation.

The water stress only explains the decreasing dew occurrence in the dry season. However, during the wet season, conditions should be more favorable for dew. In future scenarios, the incoming moisture is expected to increase (Baker and Spracklen, 2022), and the amplitude of the diurnal temperature

seems to increase (Lindvall and Svensson, 2015). Moreover, fewer precipitation days seem to be more favorable for dew occurrence since dew is more likely to form. Nevertheless, there is still an expected decrease in estimated dew days. Therefore, there must be additional factors for the projected decline. One reason could be a later transition from dry to wet season (Baker and Spracklen, 2019; Malhi et al., 2009; Marengo and Abril, 2006). The shift may be caused by less access to deep water supply, resulting in an altered water cycle due to logging (Baker and Spracklen, 2019; Marengo and Abril, 2006). Less evapotranspiration causes a higher proportion of sensible heat at the expense of latent heat (Marengo and Abril, 2006). Besides other factors, alterations in the water cycle may induce an extension of the dry season.

Figure 21b illustrates that rainy days decrease less in the first half of the wet season (DJF) in comparison to the second half (MAM), which is in opposite with the extension of the dry season in the eastern Amazon (Malhi et al., 2009). The extension of the dry season, however, is linked to deforestation (Baker and Spracklen, 2019), and models lack in a proper adjustment to land use change (Baker and Spracklen, 2022). Our results are probably not strongly influenced by this effect, but the latter may account for a fraction of the decrease in dew frequency.

Another possible explanation lies in the future elevation of the carbon dioxide concentration. A higher CO<sub>2</sub> concentration influences the stomata activity and leads to less transpiration (Malhi et al., 2009). In the Amazon, evapotranspiration is coupled to the precipitation rate. Both, the evapotranspiration rate and the precipitation recycling rate, are expected to decrease (Baker and Spracklen, 2022). Evapotranspiration within the Amazon can contribute by around 20% to its annual rainfall (Staal et al., 2018). The precipitation recycling rate in the wet season is not as high as by the end of the dry season (Fig 20c), but still influences the water availability in the Amazon (Staal et al., 2018). With a decrease in the recycling of water, some areas may show a depletion in soil moisture. This can decrease the Amazonian bulk estimate in the number of dew days. On the other hand, less transpiration affects temperature by decreasing latent heat and, therefore, increasing sensible heat. Sensible heat causes warmer temperatures, but it mainly affects temperatures during the day. Higher daytime temperatures can lead to a higher amplitude in the diurnal temperature cycle which coincides with the projections of Lindvall and Svensson (2015). This condition, however, is more favorable for dew formation.

It can be concluded that the Amazon forest is a very complex system, and it is difficult to assess changes properly. Two possibilities of CO<sub>2</sub> fertilization that may affect the results of this study are a decrease in evapotranspiration and precipitation recycling rates as well as a higher amplitude of diurnal temperatures (Lindvall and Svensson, 2015). These may affect the results, positive or negative,

respectively.

In summary, the decrease in dew days is likely due to warmer conditions, but deviations between the wet and dry seasons are likely explained differently. To a major part, increasing CO<sub>2</sub> concentrations may be a potential driver of decreasing dew days. Increasing CO<sub>2</sub> causes either warming of the air in the dry season or less transpiration (Malhi et al., 2009) due to the CO<sub>2</sub> fertilization effect in the wet season. The ecohydrologic response to elevated CO<sub>2</sub> may increase atmospheric drying (Malhi et al., 2009). Since the Amazon forest is a complex system, it is challenging to properly assess the effect on the changes in the estimated number of dew days.

## 4 Conclusion

The estimated dew days increase globally with time (Fig. 9). However, the resulting increase in estimated dew days is not entirely robust regarding the six models since ACCESS-CM2 projects a global decrease in the number of estimated dew days. Moreover, for most models, the increase is mainly due to the rise in the number of days when dew forming is possible. The counted days increase by either increasing days with temperatures above freezing point or increasing days without precipitation. The differences between the modeled trends cause the multi-model mean to even out and show no robustness regarding global estimated dew days when considering the relative frequency of dew days. The increasing temperature influences the global trend more than precipitation. This probably is due to a global increase in temperature (Allan et al., 2021). In contrast, precipitation is influenced by multiple factors and does not globally increase since it is changing differently on a regional scale (Allan et al., 2021). The high increase in the number of counted days primarily affects the north mid and high latitudes. In high latitudes, dew occurrence possibly may be at the expense of frost days.

Even though the global trends for estimated dew days are not robust, there are clear tendencies to either decrease or increase on a regional scale. The models disagree in large parts of the world. However, it can be said that the declining prediction in estimated dew days is robust in the tropics (such as the Amazon, Congo Basin, and part of South East Asia), as well as the increase in the northern subpolar and polar regions. A bias of temperature or precipitation may partly influence differences in models in the initial state (Döscher et al., 2022; Bi et al., 2020; Dunn et al., 2017; Wu et al., 2019; Cherchi et al., 2019). Both variables influence dew formation to a certain extent. Temperature directly influences the definition of dew point temperature (Eq. 5) and the here defined condition for dew formation ( $tas - 1.6^{\circ}\text{C} \leq td$ ; c.2). Precipitation indirectly influences the estimated number of dew days in combination with temperature increase.

The increase in estimated dew days in most parts north of 45°N is robust regarding the six models

(Fig. 11); however, the increase in estimated dew days in parts of subpolar Eurasia originates from a higher amount of counted days (Fig. 12). Most models show a decrease in estimated dew days when this factor is eliminated. The decrease could originate in lower relative humidity in period 2 (2070-2100) compared to period 1 (1950-1980). The robust increase in North Asia and North America seems to be due to an increase in relative humidity. In the tropics, especially the Amazon, the decrease is robust.

In fact, the strongest decline of the zonal mean of the estimated dew days is projected at the tropics (Fig. 15). Drying of the atmosphere likely causes the decrease. High latitudes in the North show the highest increase in estimated dew days. These regions may benefit from a decrease in relative humidity (Byrne and O’Gorman, 2016). The lower relative humidity in the atmosphere enhances surface cooling, which is favorable for dew formation (Ritter et al., 2019; Vuollekoski et al., 2015). It can be concluded, that most zonal regions change, but the tropics and high latitudes are more sensitive.

Generally, in the North, estimated dew days increase partly influenced by different biomes (Fig. 17). In the tundra, regions of the extratropical forest, and regions of grass and crops, the estimated number of dew days is expected to increase from 1950-1980 to 2070-2100 due to wetter conditions. Besides a higher amount of precipitation, the evapotranspiration rate increases (Scheff and Frierson, 2015). In the biome of extratropical forest, the projected dew days are more sensitive to an increasing number of days with temperatures above 0°C. The increasing future temperature seems to affect the minimum temperature more than other biomes. It affects the nightly surface cooling negatively (Staal et al., 2018).

In the present climate, dew contributes a substantial amount of water to crops (Chowdhury et al., 1990; Xiao et al., 2009). The projected increase in the number of dew days in grass and cropland is an additional water source. Besides the positive effect on the water supply, the increase may impact crop yield negatively. The water film can enhance pests and diseases in plants and, thus, can cause an increased need for pesticides (Bhardwaj et al., 2009; Nath, 2021). Pesticides, and other toxins decrease soil quality, contaminate drinking water and affect humans’ health (Houtman, 2010). Moreover, dew deludes pesticides, toxins, and fertilizer (Saab et al., 2017). It can lead to more frequent crop failures and may enhance global food shortage.

Sparsely vegetated areas are differently affected by the change. The increase in estimated dew days in the Taklimakan Desert is not equally supported by in situ studies. Also, in dry regions of sparse vegetation, models seem to have difficulties properly predicting water availability in some parts. The drier atmospheric conditions in areas of semiarid ecosystems (Feng and Fu, 2013; Jensen et al., 2019) cause a decrease in estimated dew days. Dry sparse vegetation shows a less strong decrease in

estimated dew days compared to semiarid ecosystems. The stronger decrease of semiarid ecosystems seems to be enhanced by the ecohydrological responses of plants to drying conditions. However, the resilience of plants in dryland and, thus, drier conditions over semiarid ecosystems is still in debate (Berg and McColl, 2021; Feng and Fu, 2013).

Reduced dew frequency in biomes such as semiarid ecosystems may amplify rising temperatures (Chowdhury et al., 1990). In the early morning, dew still is present on surfaces, but due to the incoming short wave radiation evaporates dew. Part of the incoming energy converts to latent heat (Bhardwaj et al., 2009), but if no dew is present, a fraction of the incoming energy may convert into sensible heat, i.e., rising temperatures. The energy budget is coupled to the water cycle. Less dew leads to lower foliar water uptake, and it even favors transpiration (Aguirre-Gutiérrez et al., 2019). It can lead to higher water uptake from the soil. Dew does not only contribute to plant water uptake but also increases soil moisture (Kidron et al., 2002; Tomaszkiwicz et al., 2017). Plants tend to reduce stomata activity when the soil moisture is depleted to reduce water loss. The reduced stomata opening decreases the transpiration rate (Malhi et al., 2009). This decreases the fraction of latent heat and can amplify rising temperatures.

Tropical forests show a robust decrease in estimated dew days (Fig. 17). This trend is noticeable in the Amazon. The region has two seasons which both show a decrease in estimated dew days, but the decrease in each season is to a different extent (Fig. 19).

In the dry season, plant water stress might be an impacting reason for reduced atmospheric humidity (Cook et al., 2020; Scheff and Frierson, 2015) and, therefore, dew formation. The decrease could be underestimated since the full potential of the plant's foliar water uptake might be underestimated (Binks et al., 2020) which would potentially enhance VPD (Berg et al., 2016).

In the wet season, the reason for the decline seems less plausible. The moisture influx is expected to increase (Baker and Spracklen, 2022) as well as days without precipitation; both are favorable for dew to form. Nevertheless, there is a decrease in estimated dew formation. The elevated CO<sub>2</sub> concentration might influence the change. Higher CO<sub>2</sub> levels in the atmosphere can cause less transpiration due to lower stomata opening (Malhi et al., 2009). Lower transpiration can negatively affect the precipitation recycling rate. Since evapotranspiration within the Amazon is recycled as precipitation by up to 20% (Staal et al., 2018), It can decrease the water availability in some areas over the Amazon. This negatively affects dew formation. On the other hand, the decrease in transpiration also seems to increase daytime temperatures (Lindvall and Svensson, 2015). This causes an increase in the amplitude of the diurnal temperature cycle, which is favorable for dew formation.

Additional factors influence dew in this complex system, making it difficult to assess the drivers of the

change. A change in the complex system due to anthropogenic forcing may lead to unexpected and irreversible change (Marengo and Abril, 2006; Malhi et al., 2009; Staal et al., 2018; Zemp et al., 2014). It can have future consequences on the system itself and the climate on a larger scale (Marengo and Abril, 2006; Malhi et al., 2009; Staal et al., 2018; Zemp et al., 2014).

Even though deforestation of the Amazon may not be well reflected in the results, it is expected to have a major impact on the resilience of the system and its impact on the water distribution over South America (Baker and Spracklen, 2019; Marengo and Abril, 2006; Malhi et al., 2009; Staal et al., 2018; Zemp et al., 2014).

## 5 Outlook

This master thesis focuses on atmospheric conditions for dew formation. The results show the importance of understanding the changes based on atmospheric conditions. However, surface conditions are a better indicator of dew formation. This master thesis includes neither dew formation within the canopy nor dew rise. Using the air surface temperature instead of skin surface temperature may lead to an underestimation of resulting dew days. Including a variable indicative of skin surface temperature would increase the study's accuracy. Predicting dew formation by air surface temperature is a limiting factor (Ritter et al., 2019); however, including observational data to test, evaluate, and correct the modeled data is a reasonable first attempt in projecting future dew frequency. Due to limited observational data in the Southern Hemisphere, the modeled data is evaluated and corrected based on the conditions in the Northern Hemisphere. Since dew is sensitive to different physical characteristics, this might result in some deviation in the Southern Hemisphere. The results could be improved if in situ studies in the Southern Hemisphere were available. The model biases affect the results to a certain extent, but results in biased areas are interpreted more cautiously. Additionally, the inter-model agreement helps to find robust changes, which is a strength of models within the CMIP archive. Including dew as a variable in the models would increase the accuracy of predicted water availability and plant resilience in the future. With a broader knowledge about dew, the future water scarcity in dry regions could be assessed more accurately.

## 6 Acknowledgment

I want to thank my supervisors, Dr. Vincent Humphrey, Dr. Erich Fischer, and Prof. Dr. Alexander Damm, for the fruitful discussions and support during my master thesis. I am grateful for the opportunity to write the thesis in the Climate physics study group, and I thank my colleagues for the interesting conversations.

We acknowledge the work of Working Group on Coupled Modelling from the World Climate Research Programme. We are thankful for the availability of the model outputs and want to thank the climate modeling groups for the work. We also thank for the access and archiving of the data to the Earth System Grid Federation (ESGF), as well as for the support of the funding agencies.



## References

- Agam, N. and Berliner, P. R., 2006. Dew formation and water vapor adsorption in semi-arid environments - A review, *Journal of Arid Environments* **65**(4).
- Aguirre-Gutiérrez, C. A., Holwerda, F., Goldsmith, G. R., Delgado, J., Yopez, E., Carbajal, N., Escoto-Rodríguez, M. and Arredondo, J. T., 2019. The importance of dew in the water balance of a continental semiarid grassland, *Journal of Arid Environments* **168**.
- Ahlström, A., Raupach, M. R., Schurgers, G., Smith, B., Arneth, A., Jung, M., Reichstein, M., Canadell, J. G., Friedlingstein, P., Jain, A. K., Kato, E., Poulter, B., Sitch, S., Stocker, B. D., Viovy, N., Wang, Y. P., Wiltshire, A., Zaehle, S. and Zeng, N., 2015. The dominant role of semi-arid ecosystems in the trend and variability of the land CO<sub>2</sub> sink, *Science* **348**(6237).
- Allan, R. P., Abramowitz, G., Adalgeirsdottir, G., Alessandri, A., Allen, R. J., Sényi, S., Raghavan, K., Renwick, J., Allan, R., Arias, P., Barlow, M., Cerezo-Mota, R., Cherchi, A., Gan, T., Gergis, J., Jiang, D., Khan, A., Pokam Mba, W., Rosenfeld, D., Tierney, J., Zolina, O., Zhai, P., Pirani, A., Connors, S., Péan, C., Berger, S., Caud, N., Chen, Y., Goldfarb, L., Gomis, M., Huang, M., Leitzell, K., Lonnoy, E., Matthews, J., Maycock, T., Waterfield, T., Yelekçi, O., Yu, R. and Zhou, B., 2021. Climate Change 2021: The Physical Science Basis (Chapter 8: Water Cycle Changes), *Technical report*.
- Baker, J. C. A. and Spracklen, D. V., 2022. Divergent Representation of Precipitation Recycling in the Amazon and the Congo in CMIP6 Models, *Geophysical Research Letters* **49**(10): e2021GL095136.  
**URL:** <https://agupubs.onlinelibrary.wiley.com/doi/abs/10.1029/2021GL095136>
- Baker, J. C., Garcia-Carreras, L., Gloor, M., Marsham, J. H., Buermann, W., Da Rocha, H. R., Nobre, A. D., De Carrioca Araujo, A. and Spracklen, D. V., 2021. Evapotranspiration in the Amazon: Spatial patterns, seasonality, and recent trends in observations, reanalysis, and climate models, *Hydrology and Earth System Sciences* **25**(4).
- Baker, J. C. and Spracklen, D. V., 2019. Climate Benefits of Intact Amazon Forests and the Biophysical Consequences of Disturbance, *Frontiers in Forests and Global Change* **2**.
- Berg, A., Findell, K., Lintner, B., Giannini, A., Seneviratne, S. I., Van Den Hurk, B., Lorenz, R., Pitman, A., Hagemann, S., Meier, A., Cheruy, F., Ducharne, A., Malyshev, S. and Milly, P. C., 2016. Land-atmosphere feedbacks amplify aridity increase over land under global warming, *Nature Climate Change* **6**(9).
- Berg, A. and McColl, K. A., 2021. No projected global drylands expansion under greenhouse warming, *Nature Climate Change* **11**(4).
- Berry, Z. C., Emery, N. C., Gotsch, S. G. and Goldsmith, G. R., 2019. Foliar water uptake: Processes, pathways, and integration into plant water budgets.
- Bhardwaj, J., Singh, S., Singh, D. and Rao, V. U., 2009. Dewfall in relation to weather variables in varying environments of mustard crop, *Journal of Agrometeorology* **11**(SPECIAL ISSUE).
- Bi, D., Dix, M., Marsland, S., O'farrell, S., Sullivan, A., Bodman, R., Law, R., Harman, I., Srbinovsky, J., Rashid, H. A., Dobrohotoff, P., Mackallah, C., Yan, H., Hirst, A., Savita, A., Dias, F. B., Woodhouse, M., Fiedler, R. and Heerdegen, A., 2020. Configuration and spin-up of ACCESS-CM2, the new generation Australian Community Climate and Earth System Simulator Coupled Model, *Journal of Southern Hemisphere Earth Systems Science* **70**(1).
- Binks, O., Coughlin, I., Mencuccini, M. and Meir, P., 2020. Equivalence of foliar water uptake and stomatal conductance?, *Plant Cell and Environment* **43**(2).
- Binks, O., Finnigan, J., Coughlin, I., Disney, M., Calders, K., Burt, A., Vicari, M. B., da Costa, A. L., Mencuccini, M. and Meir, P., 2021. Canopy wetness in the Eastern Amazon, *Agricultural and Forest Meteorology* **297**.
- Binks, O., Mencuccini, M., Rowland, L., da Costa, A. C., de Carvalho, C. J. R., Bittencourt, P., Eller, C., Teodoro, G. S., Carvalho, E. J. M., Soza, A., Ferreira, L., Vasconcelos, S. S., Oliveira, R. and Meir, P., 2019. Foliar water uptake in Amazonian trees: Evidence and consequences, *Global Change Biology* **25**(8).
- Byrne, M. P. and O'Gorman, P. A., 2013. Link between land-ocean warming contrast and surface relative humidities in simulations with coupled climate models, *Geophysical Research Letters* **40**(19).
- Byrne, M. P. and O'Gorman, P. A., 2016. Understanding decreases in land relative humidity with global warming: Conceptual model and GCM simulations, *Journal of Climate* **29**(24).

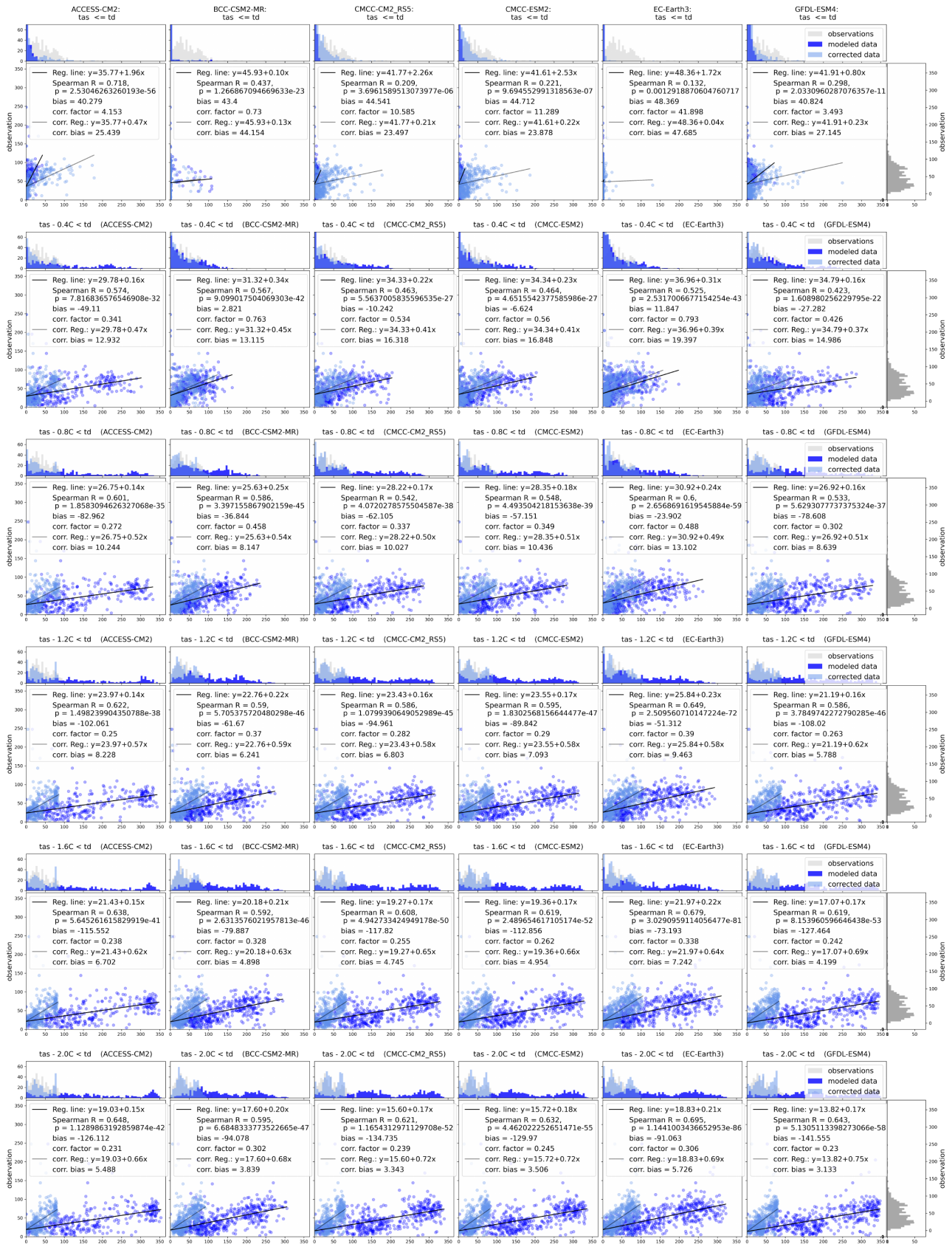
- Cherchi, A., Fogli, P. G., Lovato, T., Peano, D., Iovino, D., Gualdi, S., Masina, S., Scoccimarro, E., Materia, S., Bellucci, A. and Navarra, A., 2019. Global Mean Climate and Main Patterns of Variability in the CMCC-CM2 Coupled Model, *Journal of Advances in Modeling Earth Systems* **11**(1).
- Chowdhury, A., Das, H. P. and Mukhopadhyzy, R. K., 1990. Distribution of dew and its importance in moisture balance for rabi crops in India, *MAUSAM* **41**(4).
- Cook, B. I., Mankin, J. S., Marvel, K., Williams, A. P., Smerdon, J. E. and Anchukaitis, K. J., 2020. Twenty-First Century Drought Projections in the CMIP6 Forcing Scenarios, *Earth's Future* **8**(6).
- Dai, A., 2006. Recent climatology, variability, and trends in global surface humidity, *Journal of Climate* **19**(15).
- Dai, A., Zhao, T. and Chen, J., 2018. Climate Change and Drought: a Precipitation and Evaporation Perspective.
- Dix, M., Bi, D., Dobrohotoff, P., Fiedler, R., Harman, I., Law, R., Mackallah, C., Marsland, S., O'Farrell, S., Rashid, H., Srbinovsky, J., Sullivan, A., Trenham, C., Vohralik, P., Watterson, I., Williams, G., Woodhouse, M., Bodman, R., Dias, F. B., Domingues, C., Hannah, N., Heerdegen, A., Savita, A., Wales, S., Allen, C., Druken, K., Evans, B., Richards, C., Ridzwan, S. M., Roberts, D., Smillie, J., Snow, K., Ward, M. and Yang, R., 2019. CSIRO-ARCCSS ACCESS-CM2 model output prepared for CMIP6 CMIP historical.  
**URL:** <https://doi.org/10.22033/ESGF/CMIP6.4271>
- Döscher, R., Acosta, M., Alessandri, A., Anthoni, P., Arsouze, T., Bergman, T., Bernardello, R., Boussetta, S., Caron, L.-P., Carver, G., Castrillo, M., Catalano, F., Cvijanovic, I., Davini, P., Dekker, E., Doblas-Reyes, F. J., Docquier, D., Echevarria, P., Fladrich, U., Fuentes-Franco, R., Gröger, M., v. Hardenberg, J., Hieronymus, J., Karami, M. P., Keskinen, J.-P., Koenigk, T., Makkonen, R., Massonnet, F., Ménégoz, M., Miller, P. A., Moreno-Chamarro, E., Nieradzki, L., van Noije, T., Nolan, P., O'Donnell, D., Ollinaho, P., van den Oord, G., Ortega, P., Prims, O. T., Ramos, A., Reerink, T., Rousset, C., Ruprich-Robert, Y., Le Sager, P., Schmith, T., Schrödner, R., Serva, F., Sicardi, V., Sloth Madsen, M., Smith, B., Tian, T., Tourigny, E., Uotila, P., Vancoppenolle, M., Wang, S., Wärlind, D., Willén, U., Wyser, K., Yang, S., Yepes-Arbós, X. and Zhang, Q., 2022. The EC-Earth3 Earth system model for the Coupled Model Intercomparison }Project 6, *Geoscientific Model Development* **15**(7): 2973–3020.  
**URL:** <https://gmd.copernicus.org/articles/15/2973/2022/>
- Dou, Y., Quan, J., Jia, X., Wang, Q. and Liu, Y., 2021. Near-Surface Warming Reduces Dew Frequency in China, *Geophysical Research Letters* **48**(7).
- Douville, H., Raghavan, K., Renwick, J., Allan, R. P., Arias, P. A., Barlow, M., Cerezo-Mota, R., Cherchi, A., Gan, T. Y., Gergis, J., Jiang, D., Khan, A., Pokam Mba, W., Rosenfeld, D., Tierney, J. and Zolina, O., 2021. Water Cycle Changes, in V. Masson-Delmotte, P. Zhai, A. Pirani, S. L. Connors, C. Péan, S. Berger, N. Caud, Y. Chen, L. Goldfarb, M. I. Gomis, M. Huang, K. Leitzell, E. Lonnoy, J. B. R. Matthews, T. K. Maycock, T. Waterfield, O. Yelekçi, R. Yu and B. Zhou (eds), *Climate Change 2021: The Physical Science Basis. Contribution of Working Group I to the Sixth Assessment Report of the Intergovernmental Panel on Climate Change*, Cambridge University Press, Cambridge, United Kingdom and New York, NY, USA, pp. 1055–1210.
- Dunn, R. J., Willett, K. M., Ciavarella, A. and Stott, P. A., 2017. Comparison of land surface humidity between observations and CMIP5 models, *Earth System Dynamics* **8**(3).
- EC-Earth Consortium (EC-Earth), 2019a. EC-Earth-Consortium EC-Earth3 model output prepared for CMIP6 CMIP historical.  
**URL:** <https://doi.org/10.22033/ESGF/CMIP6.4700>
- EC-Earth Consortium (EC-Earth), 2019b. EC-Earth-Consortium EC-Earth3 model output prepared for CMIP6 ScenarioMIP ssp585.  
**URL:** <https://doi.org/10.22033/ESGF/CMIP6.4912>
- Eyring, V., Bony, S., Meehl, G. A., Senior, C. A., Stevens, B., Stouffer, R. J. and Taylor, K. E., 2016. Overview of the Coupled Model Intercomparison Project Phase 6 (CMIP6) experimental design and organization, *Geoscientific Model Development* **9**(5).
- Feng, S. and Fu, Q., 2013. Expansion of global drylands under a warming climate, *Atmospheric Chemistry and Physics* **13**(19).
- Feng, T., Zhang, L., Chen, Q., Ma, Z., Wang, H., Shangguan, Z., Wang, L. and He, J. S., 2021. Dew formation reduction in global warming experiments and the potential consequences, *Journal of Hydrology* **593**.
- Friedl, M. and Sulla-Menashe, D., 2015. MCD12C1 MODIS/Terra+Aqua Land Cover Type Yearly L3 Global 0.05Deg CMG V006.

- Garratt, J. R. and Segal, M., 1988. On the contribution of atmospheric moisture to dew formation, *Boundary-Layer Meteorology* **45**(3): 209–236.  
**URL:** <https://doi.org/10.1007/BF01066671>
- Hao, X. M., Li, C., Guo, B., Ma, J. X., Ayup, M. and Chen, Z. S., 2012. Dew formation and its long-term trend in a desert riparian forest ecosystem on the eastern edge of the taklimakan desert in China, *Journal of Hydrology* **472-473**.
- Hasler, N. and Avissar, R., 2007. What controls evapotranspiration in the Amazon basin?, *Journal of Hydrometeorology* **8**(3).
- Houtman, C. J., 2010. Emerging contaminants in surface waters and their relevance for the production of drinking water in Europe, *Journal of Integrative Environmental Sciences* **7**(4): 271–295.  
**URL:** <https://doi.org/10.1080/1943815X.2010.511648>
- Humphrey, V., Berg, A., Ciais, P., Gentine, P., Jung, M., Reichstein, M., Seneviratne, S. I. and Frankenberg, C., 2021. Soil moisture-atmosphere feedback dominates land carbon uptake variability, *Nature* **592**(7852).
- IPCC, 2021. *Climate Change 2021: The Physical Science Basis. Contribution of Working Group I to the Sixth Assessment Report of the Intergovernmental Panel on Climate Change*, Vol. In Press, Cambridge University Press, Cambridge, United Kingdom and New York, NY, USA.
- Jensen, L., Eicker, A., Dobslaw, H., Stacke, T. and Humphrey, V., 2019. Long-Term Wetting and Drying Trends in Land Water Storage Derived From GRACE and CMIP5 Models, *Journal of Geophysical Research: Atmospheres* **124**(17-18).
- John, J. G., Blanton, C., McHugh, C., Radhakrishnan, A., Rand, K., Vahlenkamp, H., Wilson, C., Zadeh, N. T., Dunne, J. P., Dussin, R., Horowitz, L. W., Krasting, J. P., Lin, P., Malyshev, S., Naik, V., Ploshay, J., Shevliakova, E., Silvers, L., Stock, C., Winton, M. and Zeng, Y., 2018. NOAA-GFDL GFDL-ESM4 model output prepared for CMIP6 ScenarioMIP ssp585.  
**URL:** <https://doi.org/10.22033/ESGF/CMIP6.8706>
- Kidron, G. J., 2000. Analysis of dew precipitation in three habitats within a small arid drainage basin, Negev Highlands, Israel, *Atmospheric Research* **55**(3-4): 257–270.
- Kidron, G. J., Herrnstadt, I. and Barzilay, E., 2002. The role of dew as a moisture source for sand microbiotic crusts in the Negev Desert, Israel, *Journal of Arid Environments* **52**(4): 517–533.
- Kidron, G. J. and Starinsky, A., 2019. Measurements and ecological implications of non-rainfall water in desert ecosystems—a review, *Ecohydrology* **12**(6).
- Krasting, J. P., John, J. G., Blanton, C., McHugh, C., Nikonov, S., Radhakrishnan, A., Rand, K., Zadeh, N. T., Balaji, V., Durachta, J., Dupuis, C., Menzel, R., Robinson, T., Underwood, S., Vahlenkamp, H., Dunne, K. A., Gauthier, P. P. G., Ginoux, P., Griffies, S. M., Hallberg, R., Harrison, M., Hurlin, W., Malyshev, S., Naik, V., Paulot, F., Paynter, D. J., Ploshay, J., Reichl, B. G., Schwarzkopf, D. M., Seman, C. J., Silvers, L., Wyman, B., Zeng, Y., Adcroft, A., Dunne, J. P., Dussin, R., Guo, H., He, J., Held, I. M., Horowitz, L. W., Lin, P., Milly, P. C. D., Shevliakova, E., Stock, C., Winton, M., Wittenberg, A. T., Xie, Y. and Zhao, M., 2018. NOAA-GFDL GFDL-ESM4 model output prepared for CMIP6 CMIP historical.  
**URL:** <https://doi.org/10.22033/ESGF/CMIP6.8597>
- Lee, J.-Y., Marotzke, J., Bala, G., Cao, L., Corti, S., Dunne, J. P., Engelbrecht, F., Fischer, E., Fyfe, J. C., Jones, C., Maycock, A., Mutemi, J., Ndiaye, O., Panickal, S. and Zhou, T., 2021. Future Global Climate: Scenario-Based Projections and Near-Term Information, in V. Masson-Delmotte, P. Zhai, A. Pirani, S. L. Connors, C. Péan, S. Berger, N. Caud, Y. Chen, L. Goldfarb, M. I. Gomis, M. Huang, K. Leitzell, E. Lonnoy, J. B. R. Matthews, T. K. Maycock, T. Waterfield, O. Yelekçi, R. Yu and B. Zhou (eds), *Climate Change 2021: The Physical Science Basis. Contribution of Working Group I to the Sixth Assessment Report of the Intergovernmental Panel on Climate Change*, Cambridge University Press, Cambridge, United Kingdom and New York, NY, USA, pp. 553–672.
- Lekouch, I., Lekouch, K., Muselli, M., Mongruel, A., Kabbachi, B. and Beysens, D., 2012. Rooftop dew, fog and rain collection in southwest Morocco and predictive dew modeling using neural networks, *Journal of Hydrology* **448-449**.
- Lindvall, J. and Svensson, G., 2015. The diurnal temperature range in the CMIP5 models, *Climate Dynamics* **44**(1): 405–421.  
**URL:** <https://doi.org/10.1007/s00382-014-2144-2>
- Lovato, T. and Peano, D., 2020a. CMCC CMCC-CM2-SR5 model output prepared for CMIP6 CMIP historical.  
**URL:** <https://doi.org/10.22033/ESGF/CMIP6.3825>

- Lovato, T. and Peano, D., 2020b. CMCC CMCC-CM2-SR5 model output prepared for CMIP6 ScenarioMIP ssp585.  
**URL:** <https://doi.org/10.22033/ESGF/CMIP6.3896>
- Lovato, T., Peano, D. and Butenschön, M., 2021a. CMCC CMCC-ESM2 model output prepared for CMIP6 CMIP historical.  
**URL:** <https://doi.org/10.22033/ESGF/CMIP6.13195>
- Lovato, T., Peano, D. and Butenschön, M., 2021b. CMCC CMCC-ESM2 model output prepared for CMIP6 ScenarioMIP ssp585.  
**URL:** <https://doi.org/10.22033/ESGF/CMIP6.13259>
- Malhi, Y., Aragão, L. E., Galbraith, D., Huntingford, C., Fisher, R., Zelazowski, P., Sitch, S., McSweeney, C. and Meir, P., 2009. Exploring the likelihood and mechanism of a climate-change-induced dieback of the Amazon rainforest, *Proceedings of the National Academy of Sciences of the United States of America* **106**(49).
- Marengo, J. A. and Abril, R., 2006. ON THE HYDROLOGICAL CYCLE OF THE AMAZON BASIN: A HISTORICAL REVIEW AND CURRENT STATE-OF-THE-ART.
- Meinshausen, M., Nicholls, Z. R., Lewis, J., Gidden, M. J., Vogel, E., Freund, M., Beyerle, U., Gessner, C., Nauels, A., Bauer, N., Canadell, J. G., Daniel, J. S., John, A., Krummel, P. B., Luderer, G., Meinshausen, N., Montzka, S. A., Rayner, P. J., Reimann, S., Smith, S. J., Van Den Berg, M., Velders, G. J., Vollmer, M. K. and Wang, R. H., 2020. The shared socio-economic pathway (SSP) greenhouse gas concentrations and their extensions to 2500, *Geoscientific Model Development* **13**(8).
- meteoblue AG, n.d.. meteoblue AG.  
**URL:** <https://content.meteoblue.com>
- Monteith, J. L. and Unsworth, M. H., 2013. Properties of Gases and Liquids, *Principles of Environmental Physics* pp. 5–23.
- Nath, S., 2021. Dew as Source of Emerging Contaminants in Agricultural System.
- O’Gorman, P. A. and Muller, C. J., 2010. How closely do changes in surface and column water vapor follow Clausius-Clapeyron scaling in climate change simulations?, *Environmental Research Letters* **5**(2).
- Pütz, T., Kiese, R., Wollschläger, U., Groh, J., Rupp, H., Zacharias, S., Priesack, E., Gerke, H. H., Gasche, R., Bens, O., Borg, E., Baessler, C., Kaiser, K., Herbrich, M., Munch, J. C., Sommer, M., Vogel, H. J., Vanderborght, J. and Vereecken, H., 2016. TERENO-SOILCan: a lysimeter-network in Germany observing soil processes and plant diversity influenced by climate change, *Environmental Earth Sciences* **75**(18).
- Ritter, F., Berkelhammer, M. and Beysens, D., 2019. Dew frequency across the US from a network of in situ radiometers, *Hydrology and Earth System Sciences* **23**(2).
- Saab, O. J., Griesang, F., Alves, K. A., Higashibara, L. R. and Genta, W., 2017. Pesticides deposition in vineyards on different conditions of leaf wetness, *Engenharia Agricola* **37**(2).
- Scheff, J. and Frierson, D. M., 2015. Terrestrial aridity and its response to greenhouse warming across CMIP5 climate models, *Journal of Climate* **28**(14).
- Sharan, G., 2007. Harvesting dew to supplement drinking water supply in arid coastal villages of Gujarat, *Indian Institute of Management Ahmedabad, Research and Publication Department, IIMA Working Papers*, pp. 13–14.
- Sherwood, S. and Fu, Q., 2014. A drier future?
- Simmons, A. J., Willett, K. M., Jones, P. D., Thorne, P. W. and Dee, D. P., 2010. Low-frequency variations in surface atmospheric humidity, temperature, and precipitation: Inferences from reanalyses and monthly gridded observational data sets, *Journal of Geophysical Research Atmospheres* **115**(1).
- Staal, A., Tuinenburg, O. A., Bosmans, J. H., Holmgren, M., Van Nes, E. H., Scheffer, M., Zemp, D. C. and Dekker, S. C., 2018. Forest-rainfall cascades buffer against drought across the Amazon, *Nature Climate Change* **8**(6).
- Sulla-Menashe, D. and Friedl, M. A., 2018. User Guide to Collection 6 MODIS Land Cover (MCD12Q1 and MCD12C1) Product.  
**URL:** <https://doi.org/10.5067/MODIS/MCD12Q1.006>
- Tetens, O., 1930. Über einige meteorologische, *Zeitschrift für Geophysik* **6**: 297–309.

- Tomaszkiewicz, M., Abou Najm, M., Zurayk, R. and El-Fadel, M., 2017. Dew as an adaptation measure to meet water demand in agriculture and reforestation, *Agricultural and Forest Meteorology* **232**: 411–421.
- Vuollekoski, H., Vogt, M., Sinclair, V. A., Duplissy, J., Järvinen, H., Kyrö, E. M., Makkonen, R., Petäjä, T., Prisle, N. L., Räisänen, P., Sipilä, M., Ylhäisi, J. and Kulmala, M., 2015. Estimates of global dew collection potential on artificial surfaces, *Hydrology and Earth System Sciences* **19**(1).
- Wang, C., Cen, Y., Liu, M. and Bowler, P., 2017. Formation and influencing factors of dew in sparse elm woods and grassland in a semi-arid area, *Acta Ecologica Sinica* **37**(3).
- Wang, Y., Liu, Y. and Jin, J., 2018. Contrast Effects of Vegetation Cover Change on Evapotranspiration during a Revegetation Period in the Poyang Lake Basin, China, *Forests* **9**(4).  
**URL:** <https://www.mdpi.com/1999-4907/9/4/217>
- Wright, S. J. and Muller-Landau, H. C., 2006. The future of tropical forest species.
- Wu, T., Chu, M., Dong, M., Fang, Y., Jie, W., Li, J., Li, W., Liu, Q., Shi, X., Xin, X., Yan, J., Zhang, F., Zhang, J., Zhang, L. and Zhang, Y., 2018a. BCC BCC-CSM2MR model output prepared for CMIP6 CMIP esm-hist.  
**URL:** <https://doi.org/10.22033/ESGF/CMIP6.2901>
- Wu, T., Chu, M., Dong, M., Fang, Y., Jie, W., Li, J., Li, W., Liu, Q., Shi, X., Xin, X., Yan, J., Zhang, F., Zhang, J., Zhang, L. and Zhang, Y., 2018b. BCC BCC-CSM2MR model output prepared for CMIP6 CMIP historical.  
**URL:** <https://doi.org/10.22033/ESGF/CMIP6.2948>
- Wu, T., Lu, Y., Fang, Y., Xin, X., Li, L., Li, W., Jie, W., Zhang, J., Liu, Y., Zhang, L., Zhang, F., Zhang, Y., Wu, F., Li, J., Chu, M., Wang, Z., Shi, X., Liu, X., Wei, M., Huang, A., Zhang, Y. and Liu, X., 2019. The Beijing Climate Center Climate System Model (BCC-CSM): the main }progress from CMIP5 to CMIP6, *Geoscientific Model Development* **12**(4): 1573–1600.  
**URL:** <https://gmd.copernicus.org/articles/12/1573/2019/>
- Xiao, H., Meissner, R., Seeger, J., Rupp, H. and Borg, H., 2009. Effect of vegetation type and growth stage on dewfall, determined with high precision weighing lysimeters at a site in northern Germany, *Journal of Hydrology* **377**(1-2): 43–49.
- Xin, X., Wu, T., Shi, X., Zhang, F., Li, J., Chu, M., Liu, Q., Yan, J., Ma, Q. and Wei, M., 2019. BCC BCC-CSM2MR model output prepared for CMIP6 ScenarioMIP ssp585.  
**URL:** <https://doi.org/10.22033/ESGF/CMIP6.3050>
- Yokoyama, G., Yasutake, D., Minami, K., Kimura, K., Marui, A., Yueru, W., Feng, J., Wang, W., Mori, M. and Kitano, M., 2021. Evaluation of the physiological significance of leaf wetting by dew as a supplemental water resource in semi-arid crop production, *Agricultural Water Management* **255**.
- Yu, R., Zhang, Z., Lu, X., Chang, I. S. and Liu, T., 2020. Variations in dew moisture regimes in desert ecosystems and their influencing factors.
- Zemp, D. C., Schleussner, C.-F., Barbosa, H. M. J., van der Ent, R. J., Donges, J. F., Heinke, J., Sampaio, G. and Rammig, A., 2014. On the importance of cascading moisture recycling in South America, *Atmospheric Chemistry and Physics* **14**(23): 13337–13359.  
**URL:** <https://acp.copernicus.org/articles/14/13337/2014/>
- Zha, T., Barr, A. G., van der Kamp, G., Black, T. A., McCaughey, J. H. and Flanagan, L. B., 2010. Interannual variation of evapotranspiration from forest and grassland ecosystems in western Canada in relation to drought, *Agricultural and Forest Meteorology* **150**(11): 1476–1484.  
**URL:** <https://www.sciencedirect.com/science/article/pii/S0168192310002030>
- Zhou, S., Park Williams, A., Berg, A. M., Cook, B. I., Zhang, Y., Hagemann, S., Lorenz, R., Seneviratne, S. I. and Gentile, P., 2019. Land-atmosphere feedbacks exacerbate concurrent soil drought and atmospheric aridity, *Proceedings of the National Academy of Sciences of the United States of America* **116**(38).

# 7 Appendices





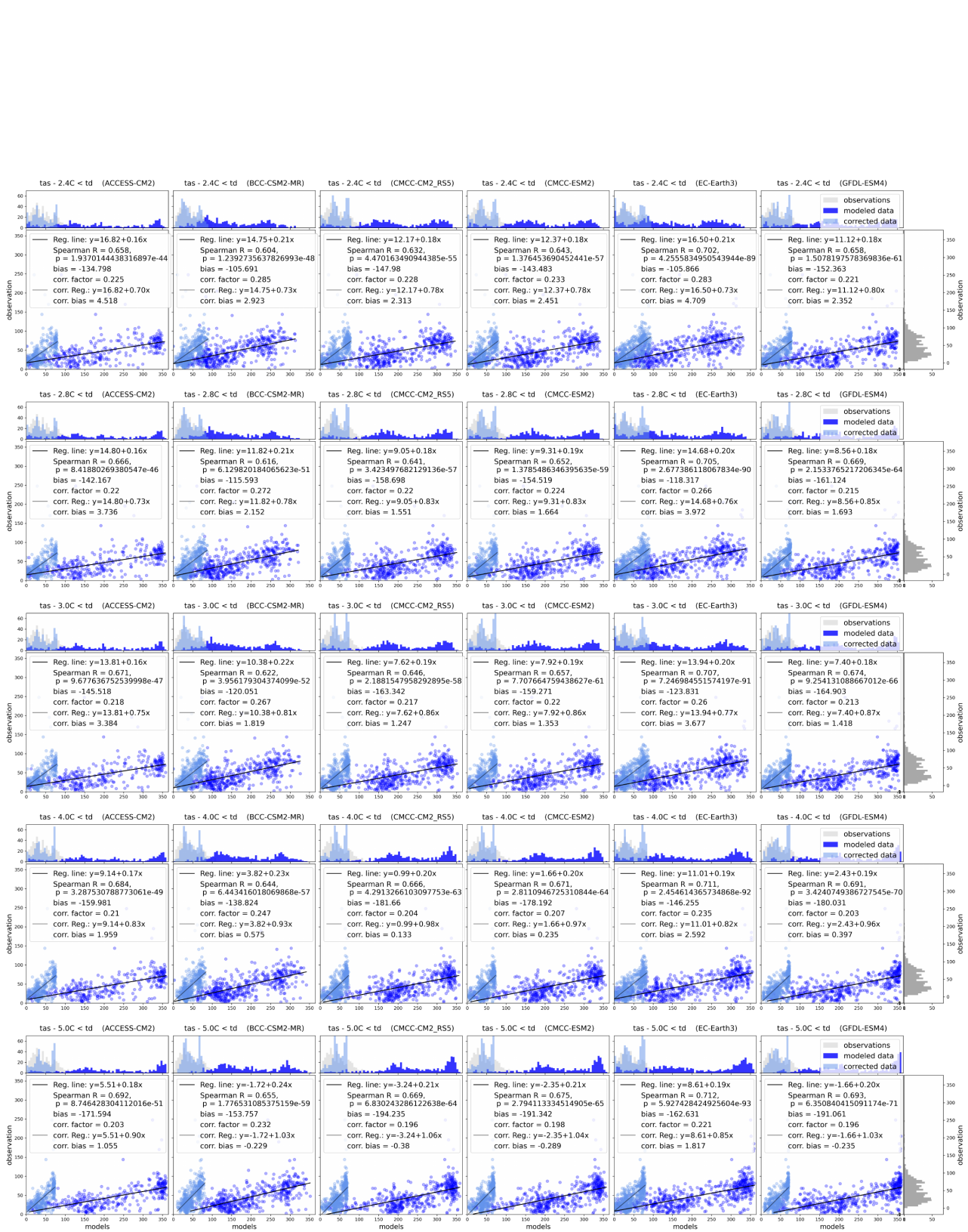


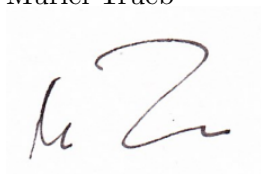
**Figure 1:** Linear regression analysis for  $tas - \alpha \leq td$  with  $x$  as model and  $y$  as observations including the histogram.  $\alpha$  is between 0.0 and 5.0 beginning with 0 on top to 5.0 at the bottom. Modeled data is shown in blue, corrected data in lighter blue, and observation in gray.

**Personal declaration**

I hereby declare that the submitted Thesis is the result of my own, independent work. All external sources are explicitly acknowledged in the Thesis.

Bern, 30. September 2022

Muriel Trüb

A handwritten signature in dark ink, appearing to read 'Muriel Trüb', is centered below the printed name. The signature is written in a cursive style with a large, looped 'M' and 'T'.